Scube2 primes Dispatched and ADAM10-mediated Shh release by recruiting HDL acceptors to the plasma membrane

J. Puschmann[1], G. Steffes[2], J. Froese[1], D. Manikowski[1], K. Ehring[1], J. Wittke[1], C. Garbers[3], S.V. Wegner[1] and K. Grobe[1#]

[1]Institute of Physiological Chemistry and Pathobiochemistry, University of Münster, Münster, Germany
[2]Institute of Neuro- and Behavioral Biology, University of Münster, Münster, Germany
[3] Institut of Clinical Biochemistry, Hannover Medical School, Hannover, Germany

 # Correspondence:
Dr. Kay Grobe, ORCID: 0000-0002-8385-5877
kgrobe@uni-muenster.de

Keywords:

A Disintegrin and Metalloproteinase 10, Hedgehog, Scube2, LPP, high-density lipoprotein, cholesterol, Dispatched.

Summary:

Hedgehog (Hh) morphogens are essential regulators of growth and patterning at considerable distances from their source, despite being produced as double lipidated proteins that attach to the outer plasma membrane (PM) leaflet of producing cells. While mechanisms to overcome this limitation include the 12-pass transmembrane protein Dispatched1 (Disp), the soluble glycoprotein Scube2, proteolytic processing of lipidated peptide termini, and soluble lipoproteins (LPPs) acting as Hh acceptors and transporters, the molecular interplay of these release factors for effective Hh solubilization from the PM remains controversial. In this work, we used in vivo functional knockdown together with in vitro experiments to show that A Disintegrin and Metalloproteinase 10, Scube2 and Disp act synergistically to remove Hh from the PM and transfer it to LPP acceptors. We also show that Scube2 requirement for Hh transfer depends on LPP acceptor levels: low LPP levels in media require Scube2 for efficient Hh release, whereas increasing LPP levels render Scube2 function increasingly dispensable. Biochemical analysis explained this observation by showing that Scube2 binds high-density LPP (HDL) via its 9 EGF domains and associates with the PM via interactions with cell surface heparan sulfate (HS), revealing a previously unknown role for Scube2 in bridging low-abundance soluble carriers for Hh with HS-rich Hh release sites.

Introduction

The Hedgehog (Hh) morphogen family plays critical roles in vertebrate and invertebrate development [1], and the vertebrate Hh family member Sonic hedgehog (Shh) also contributes to the progression of several cancers [2-4]. Understanding the conserved mechanisms that characterize Hh signaling is therefore of great importance. The first conserved mechanism unique to the Hh pathway is that Hh production begins with the autocatalytic covalent attachment of a cholesteryl moiety to the C-terminal glycine of the 19kDa Hh signaling domain [5]. In a subsequent step, Hh acyltransferase (Hhat) adds a palmitate to the free N-amino group of cholesteroylated Hhs [6], resulting in dual-lipidated morphogens that remain tightly bound to the surface of the producing cell upon secretion. The dual-lipidated proteins then bind to heparan sulfate (HS) proteoglycans (HSPGs) on the cell surface to form large, light-microscopically visible signaling platforms [7]. HSPGs are highly abundant extracellular molecules expressed in most vertebrate and invertebrate cell types and consist of plasma membrane (PM)-associated core proteins to which multiple HS chains are attached. The HS chains (as well as that of heparin, a highly sulfated form of HS) consist of numerous glucuronic acid and N-acetylglucosamine repeats that are modified by sulfotransferases and a glucuronic acid-C5 epimerase to form linear, highly negatively charged polymers that interact with numerous extracellular proteins, including all vertebrate and invertebrate Hh family members, via reversible electrostatic interactions. These interactions at the PM influence Hh bioactivity [8-12], first by assembling HS-bound lipid-modified Hh into the punctate signaling platforms on the cell surface [7, 13], and second by recruiting soluble proteins to these HS-rich platforms to regulate Hh release [14-16].

A soluble protein known to bind HS on the cell-surface to enhance Shh release up to 10-fold [17-20] is Scube2 (signal sequence, cubulin (CUB) domain, epidermal growth factor (EGF)-like protein 2) [16, 21-23]. In addition to its Shh releasing activity, Scube2 is also known to form homocomplexes or heterocomplexes with the other Scube family members 1 and 3, bone morphogenetic protein (BMP), E-cadherin or VEGF-A165 and VEGFR2 (summarized in [24]). Scube2 consists of a signal sequence followed by nine EGF domains, a spacer region, a cysteine-rich domain (CRD) and a C-terminal CUB domain. In general, CUB domains regulate biological processes such as developmental patterning [25] and signal transduction [26], usually by supporting protein-protein interactions [27], and EGF domains usually function in homophilic or heterophilic protein interactions [28, 29], such as with growth factors, to modulate their signaling activity [30, 31]. The spacer region separating the EGF domains from the CRD and CUB domains contains the HS binding sites [32].

Another Hh release protein at the PM is Dispatched1 (Disp) [33-37]. Disp is composed of 12 transmembrane helices and two extracellular domains, making it a member of the resistance-nodulation-division (RND) family of transmembrane efflux pumps. These pumps typically maintain cellular homeostasis by expelling toxic substances. In addition, Disp contains a conserved multi-pass transmembrane region known as the sterol sensing domain (SSD), which, in other SSD-containing proteins, is involved in the regulation of free and esterified cholesterol levels in cells or their transport [38]. The SSD motif in Disp therefore suggests that Disp binds to PM cholesterol and possibly transports it out of the cell. Indeed, such a transporter function for free cholesterol from the PM to high-density lipoproteins (HDL) has recently been confirmed [33] and is consistent with HDL serving as a well-established soluble acceptor for peripheral cholesterol [39]. Such a cholesterol acceptor function of HDLs is made possible by their small

size of 5-10 nm, which makes them abundant not only in the circulation but also in interstitial fluids, both in the adult and during development [40]. In addition, Disp has recently been shown to extract the C-terminally linked Shh sterol to transfer it from the cell surface to HDL [41]. To complete this halfway transfer of Shh to HDL, the palmitoylated N-terminal membrane anchor is cleaved, most likely by a cell surface-associated protease (a sheddase) [42-44]. Alternatively, an earlier model proposed that Disp extracts dual-lipidated Hh from the PM and delivers it to Scube2 [21, 22], which then transports Hh away from the producing cell.

To learn more about the interplay between these Hh release proteins and their modes of function, we used a bicistronic Hhat/Shh coexpression system [23] that avoids the artifacts of Shh overexpression by quantitatively producing dual lipidated Shh in HEK293 (human embryonic kidney) cells and in cells knocked out for either Disp function or the function of the cell surface sheddases A disintegrin and metalloproteinase 10 (A10) and A17. We then analyzed cellular and solubilized Shh by biochemical and biophysical methods and *in vivo*. These experiments revealed that A10 is the major Shh sheddase in HEK293 cells and that the *Drosophila* ortholog of A10, Kuzbanian (Kuz), is essential for unimpaired Hh-regulated fly eye development. To learn more about the role of Scube2 in A10-mediated Shh release, we immunoprecipitated Scube2 and analyzed interacting extracellular proteins by mass spectrometry. This revealed that Scube2 binds to numerous proteases, protease inhibitors and, importantly, to ApoA1, the immobile apoprotein typical of HDL. Scube2 immunoprecipitation followed by immunoblotting confirmed tight Scube2/HDL interactions. We also observed that increasing HDL levels in serum-free media strongly enhanced Shh solubilization from transfected HEK293 cells, while rendering Scube2 increasingly dispensable. Together, these findings revealed a previously unsuspected role for Scube2 in binding low abundant soluble HDL and, via its established affinity for cell surface HS, in recruiting the soluble LPP carrier to the PM to enhance Disp- and A10-mediated Shh release. These findings are consistent with and integrate published *in vivo* data on the essential function of Disp in Hh release [34-37], on the purely modulatory functions of Scube2 *in vivo* [17, 18, 45], on the requirement of LPPs for Hh release in flies [40, 46], and on the association of Hh into “large punctate” soluble structures that likely represent soluble Hh-LPP complexes [47-50].

Results:

A10 sheds dual-lipidated Shh from the PM

To compensate for potential drawbacks of protein overexpression experiments, such as missing or insufficient post-translational protein lipidation and thus altered protein function, we routinely express Shh together with Hhat from the same bicistronic mRNA and monitor complete Hh lipidation by reverse phase high pressure liquid chromatography (RP-HPLC). This strategy ensures consistent quantitative dual lipidation of cell surface-associated Shh. 36 h post-transfection, media containing 10% serum was changed to serum-free DMEM and Shh was solubilized for 6 h. Notably, HEK293 cells were not washed between media changes to leave residual traces of serum in the assay. We refer to this experimental condition as “serum-depleted” throughout this paper. We then used SDS-PAGE/Western blotting to compare solubilized Shh from TCA-precipitated media (m) with the cellular Shh precursor (c) and also to

directly compare Shh solubilization from cells expressing Disp (HEK) or not (Disp$^{-/-}$) [33] (Figure 1A). As shown previously [41], Shh release from Disp$^{-/-}$ cells was strongly decreased compared to HEK cells expressing Disp, and maximal Shh release required the presence of Scube2 (Figure 1B, Supplementary Figure1A shows loading and specificity controls on the same stripped blot, Figure 1B', B'' shows quantification of Disp- and Scube2-dependent Shh release). This result was consistent with the known synergistic roles of Disp and Scube2 in Shh release. Importantly, we also observed an electrophoretic mobility shift when soluble Shh (Figure 1B, arrowhead) was compared with the corresponding membrane-bound precursor (asterisk). This result suggests that the dual-lipidated, PM-associated Shh is not simply "extracted" from the cell, as this would not have changed its electrophoretic mobility. Instead, previous side-by-side analysis of cellular and solubilized Shh by RP-HPLC showed that the observed mobility shift was caused by proteolytic removal of terminal peptide anchors during Shh release [41]. This prompted us to ask which sheddase catalyzes the truncation and release of Shh from Disp- and Scube2-producing cells, and whether proteolytic processing of Hh could also be detected *in vivo*.

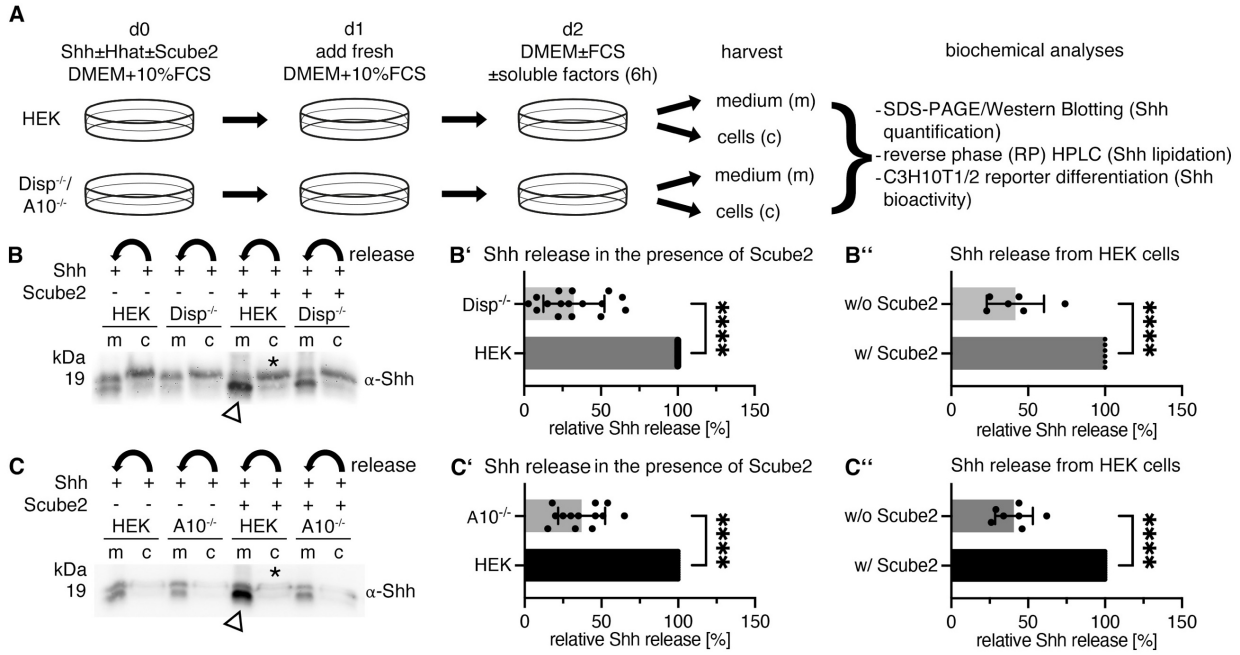

Figure 1: Scube2-mediated Shh solubilization requires Disp and A10. A) Experimental setup. HEK293 cells with or without Disp and A10 function were co-transfected with Shh/Hhat and in the presence or absence of Scube2. Cells were grown in DMEM containing 10% FCS for a total of 36 hours before serum-containing medium was aspirated and fresh medium without serum was added for 6 hours (serum-depleted conditions). Proteins secreted into the media were TCA precipitated and the corresponding cells were lysed directly on the plate for subsequent analysis by SDS-PAGE/immunoblotting or RP-HPLC. **B)** Shh solubilization from Disp-expressing HEK cells (arrowhead) requires Scube2, and Shh release from Disp$^{-/-}$ cells is severely impaired. m: media, c: Shh from the corresponding cell lysate (asterisk). Bent arrows indicate Shh solubilization from cells into corresponding media in this and in all subsequent experiments. See Supplementary Figure1A for specificity and loading controls. **B')** Quantification of relative Shh release from HEK and Disp$^{-/-}$ cells in the presence of Scube2. Only solubilized Shh with increased electrophoretic mobility (lower bands) was quantified using ImageJ.

Signals from cells expressing Shh together with Disp and Scube2 were set to 100%. Unpaired t-test, two-tailed. ****: $p<0.0001$, n=16. **B'')** Quantification of Shh release from HEK cells in the presence or absence of Scube2. Shh and Scube2 expressing cells (referred to as "w/Scube2") were set to 100%. Unpaired t-test, two-tailed. ****: $p<0.0001$, n=6. **C)** A10 and Scube2 also enhance the conversion of dually lipidated cellular Shh (asterisk) into a truncated soluble form (arrowhead). **C')** Quantification of Shh release from A10-expressing HEK cells and from $A10^{-/-}$ cells. Shh release from HEK cells was set to 100%. Unpaired t-test, two-tailed. ****: $p<0.0001$, n=13. **C'')** Quantification of Shh release from HEK cells expressing A10 in the presence or absence of Scube2. HEK cells expressing Scube2 were set to 100%. Unpaired t-test, two-tailed. ****: $p<0.0001$, n=7. See Supplementary Table 1 for detailed statistical information.

To address this question, we analyzed the release of dual-lipidated, PM-associated Shh from Disp-expressing and A10-expressing HEK cells and from Disp-expressing cells rendered A10 deficient by CRISPR/Cas9 (hereafter referred to as $A10^{-/-}$ cells). We observed that Shh solubilization from $A10^{-/-}$ cells in serum-depleted media was reduced to a similar extent as that observed for $Disp^{-/-}$ cells, even in the presence of Scube2 (Figure 1C, Supplementary Figure1B). These results demonstrate that Disp and Scube2 are not sufficient for maximal Shh release from HEK293 cells, as A10 is an essential contributor to this process (Figure 1C', C''). As described previously [33, 41], we observed an electrophoretic mobility shift of A10-solubilized Shh (Figure 1C, arrowhead) compared to the corresponding cellular forms (asterisk), which can now be clearly attributed to A10 activity during Shh release. RP-HPLC of the cellular and solubilized material shown in Figure 1C (indicated by the asterisk and arrowhead, respectively) confirmed that A10 removed the lipidated Shh peptide termini during solubilization (Supplementary Figure 1C). In contrast to A10, the closely related protease A17/TACE did not significantly contribute to Shh solubilization under the same experimental conditions (Supplementary Figure 1D).

We next examined whether an artificially monolipidated ^{C25S}Shh variant lacking the N-terminal palmitate and a ShhN variant lacking the C-terminal cholesterol were also specifically released from A10 expressing HEK293 cells (Figure 2A,B, Supplementary Figure 1E,F). We again monitored the proteolytic processing of both variants during release and found that the release of truncated ^{C25S}Shh was enhanced by A10 and Scube2 (Figure 2A, A', A''), but somewhat less A10 controlled than that of dual lipidated Shh (Figure 1C-C''). A second unprocessed form, represented by the upper (lower electrophoretic mobility) band, was released in an A10- and Scube2-independent manner. Proteolytic processing and release of ShhN was not controlled by either A10 or Scube2 (Figure 2B' B''), suggesting that more than one sheddase can cleave the ShhN N-terminus under non-specific conditions (i.e. conditions lacking dual Shh lipidation and Scube2 or A10). Indeed, the level of control of ShhN solubilization is similar to that of ^{C25S}ShhN, a non-lipidated soluble control protein (Figure 2C-C'', Supplementary Figure 1G). Taken together, these results demonstrate that A10, but not A17, is a major contributor to Disp- and Scube2-mediated Shh release from HEK293 cells in serum-depleted media. When one of the three components is missing, Shh release is severely reduced, suggesting that the three proteins cooperate in Shh release. Our results also show that both Shh lipids must be present for the release of cell surface-associated recombinant Shh to be strictly controlled by A10-, Scube2 and Disp.

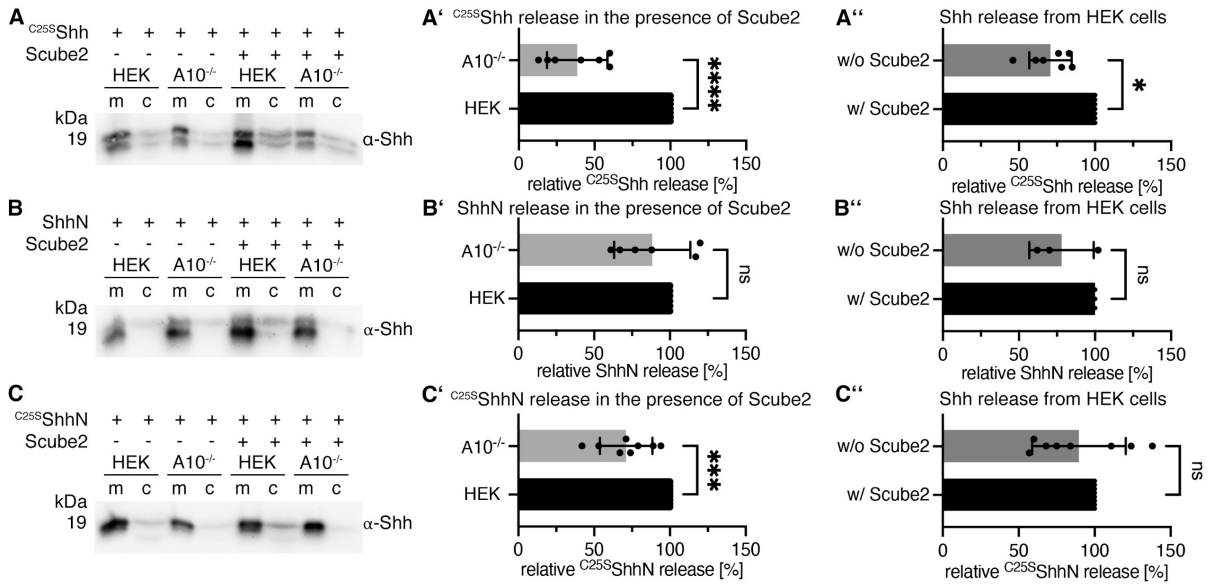

Figure 2: A10 and Scube2 differentially control the release of artificial non- and monolipidated Shh variants. A-C) Solubilization of non-palmitoylated ^{C25S}Shh, non-cholesteroylated ShhN and non-lipidated ^{C25S}ShhN in serum-depleted media. ^{C25S}Shh release remains associated with A10 function but is less controlled by Scube2. ShhN release is independent of A10 and Scube2, as is the solubilization of the ^{C25S}ShhN control. **A'-C')** Protein quantification from HEK cells or A10$^{-/-}$ cells in the presence of Scube2. Shh signals from HEK cells also expressing Scube2 were set to 100%. Unpaired t-test, two-tailed. ns: p>0.05, ****: p<0.0001, n=7 (A'), n=6 (B'), n=8 (C'). **A''-C'')** Quantification of protein solubilization from HEK cells in the presence or absence of Scube2. Shh signals from HEK cells also expressing Scube2 were set to 100%. Unpaired t-test, two-tailed. ns: p>0.05, *: p<0.05, n=7 (A''), n=3 (B''), n=8 (C''). See Supplementary Table 1 for detailed statistical information.

Tissue-specific depletion of Hh, Disp and the A10 ortholog Kuz results in similar phenotypes in the *Drosophila* eye

Next, we tested our *in vitro* results on A10-mediated Hh solubilization *in vivo*. To this end, we investigated the A10 ortholog Kuzbanian (Kuz) and its possible contribution to Hh-regulated *Drosophila* eye development. The adult *Drosophila* eye is a honeycomb matrix of ~700 photoreceptors (ommatidia) that develop in a wave of differentiation that moves from the posterior to the anterior of the eye disc, called the morphogenetic furrow (Figure 3A). Cells anterior to the furrow respond to Hh released by cells posterior to the furrow by eventually producing and releasing the same protein. This creates a cyclic, short-range Hh signaling mode that drives the furrow across the disc [41, 51] and determines the number of ommatidia in the adult eye: Impaired Hh release during development results in fewer ommatidia. Another advantage of using eye development as an experimental system is that it is not essential for fly survival. This allowed us to use the adult eye as a convenient and reliable readout for impaired Hh biofunction, while avoiding the expected deleterious pleiotropic effects of Kuz knockdown in other developing tissues. We used the established eye disc-specific GMR (glass multimer reporter)-Gal4 driver [52] to express dominant-negative Kuz^{DN} proteins under upstream activating sequence (UAS)-control to suppress endogenous Kuz function in the developing eye

[53], and hypothesized that this should impair the release and reduce the biofunction of endogenously produced Hh. While we found that GMR-controlled Kuz^{DN} expression at 25°C mostly resulted in pupal lethality, probably due to leaky Kuz^{DN} expression in other tissues besides the eye disc, we also found that surviving flies had significantly reduced numbers of ommatidia (n=235±22 ommatidia/eye compared to GFP-expressing positive control discs that formed eyes consisting of n=657±38 ommatidia, n=10 eyes were analyzed for each line, p<0.0001, Figure 3B,C). We often observed an additional "rough eye" phenotype upon GMR-GAL4-driven Kuz^{DN} expression, especially at lower temperatures (Supplementary Figure 1H). This additional phenotype is likely caused by impaired Notch signaling, consistent with the known dependence of Notch lateral inhibition of photoreceptor development on Kuz [53]. Another established specificity control for the small eye phenotype are homozygous hh^{bar3} eye discs that lack sufficient Hh expression to drive furrow progression (270±28 ommatidia, n=10 eyes analyzed, p=0.1 when compared to GMR>Kuz^{DN} eyes, Figure 3B,C) [54]. This particular result is noteworthy because it shows that impairing the activity of endogenous Kuz affects Hh-driven *Drosophila* eye development to a similar extent as the well-established Hh^{bar3} mutation. Along the same line, eye disc-specific clonal replacement of endogenous disp with the hypomorphic allele $disp^{S037707}$ ($disp^{LacW}$) [34] under eyFlp3.5 control also impaired eye development (304±58 ommatidia, n=10 eyes analyzed, p=0.0004 when compared to GMR>kuz^{DN} eyes, Figure 3B,C), mirroring our *in vitro* finding that both A10 knockout and Disp knockout in HEK cells impair Shh release to a similar extent. Finally, expression of cleavage-resistant ^{HA}Hh under the same GMR-Gal4 control in eye discs lacking most endogenous Hh also resulted in a small eye phenotype (n=244±22 ommatidia, n=10 eyes analyzed, p=0.97 when compared to GMR>Kuz^{DN}, Figure 3B,C), confirming previous results [41, 55]. Since this very similar phenotype is specifically caused by impaired N-terminal Hh cleavage due to the inserted HA tag, we suggest that impaired Notch function is unlikely to have caused the small eye phenotype as a consequence of Kuz^{DN} expression.

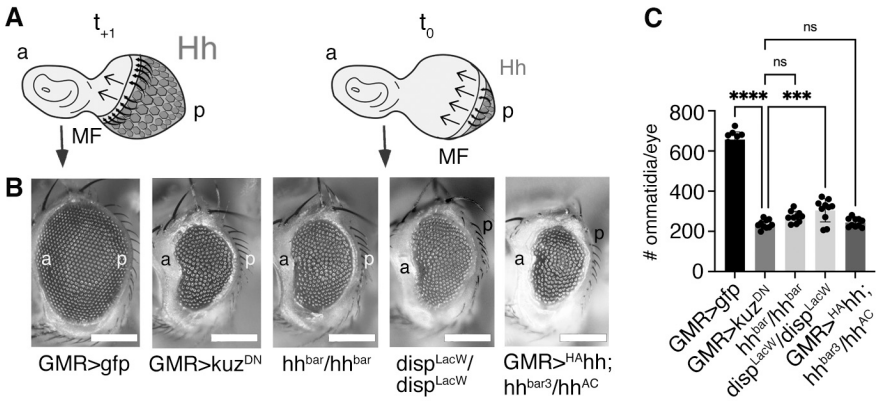

Figure 3: Disruption of endogenous Kuz biofunction impairs Hh-regulated eye development *in vivo*. A) The cartoon shows short-range Hh signaling in the part of the *Drosophila* eye disc that gives rise to the compound eye. Reiterated cell-to-cell Hh signaling from a mobile source moving from posterior (p) to anterior (a) (called the morphogenetic furrow (MF)) drives photoreceptor (hexagon) differentiation across the eye primordium. The rate of MF movement over time ($t_0 \rightarrow t_{+1}$) is Hh-dependent and ultimately determines the number of photoreceptors (ommatidia) in the adult *Drosophila* eye. Black curved arrows

indicate short-range Hh spreading, large straight arrows indicate MF movement. The posterior GMR expression domain where endogenous Kuz activity is reduced is shown in gray. **B)** Flies expressing GFP under eye-disc specific GMR-control served as positive controls (left). GMR-mediated suppression of endogenous Kuz biofunction severely impairs eye development. Negative control discs, which lack most Hh expression due to a promoter mutation that specifically affects eye development (hh^{bar3}/hh^{bar3}), discs defective in Hh release in clonal disc tissue due to an eyFlp3.5-driven exchange of disp with the hypomorphic allele $disp^{S037707}$ ($disp^{LacW}$), and discs expressing ^{HA}Hh proteins with the N-terminal Kuz processing site replaced by an HA tag under GMR control in eye discs lacking endogenous Hh (hh^{bar3}/hh^{AC}) also develop small kidney-shaped eyes. Scale bars: 100 µm. **C)** Quantification of phenotypes. One-way ANOVA, Sidak's multiple comparison test. ****: p<0.0001, ***: p=0.004, n.s.>0.1, n=10 for all genotypes. See Supplementary Table 1 for detailed statistical information.

Scube2 specifically enhances the A10-mediated processing and release of Shh, but not the general activity of A10

Does Scube2 specifically enhance Shh solubilization by A10, or does Scube2 activate A10 in a more general manner? To address this question, we tested the ability of Scube2 to activate proteolytic processing of the well-established A10 substrate interleukin-2 receptor α (myc-tagged IL-2Rα in our assays) [56] by analyzing ligand solubilization from transfected HEK cells and $A10^{-/-}$ cells using the same experimental design as described above (Figure 4A, A', Supplementary Figure 2A). We confirmed that IL-2Rα shedding is A10 dependent, as $A10^{-/-}$ cells released almost no receptor into the media. However, similar IL-2Rα release was observed from control cells regardless of the presence or absence of Scube2 (Figure 4A, A'). Similar results were obtained for another established A10 substrate, the IL-6Rα (Supplementary Figure 2B, B') [57, 58]. Based on these results, we conclude that Scube2 does not act as a general enhancer of A10 activity. Instead, Scube2 acts specifically on A10 processing of its substrate Shh at the PM. The specific requirement of Disp and Scube2 for A10-mediated Shh processing provides an unexpected example of how the substrate specificity of an otherwise promiscuous protease [59, 60] can be effectively controlled, and prompted us to investigate the underlying mechanisms of sheddase-mediated Shh release.

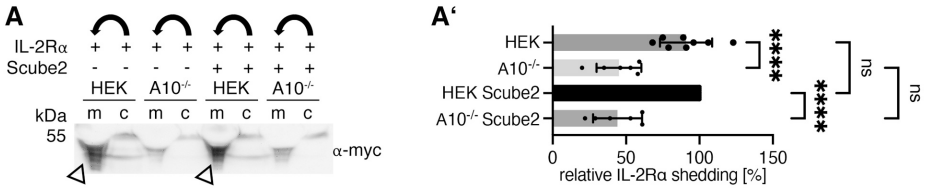

Figure 4: Scube2 is not a general enhancer of A10 shedding activity. A) HEK cells and $A10^{-/-}$ cells were transfected with the established A10 target IL-2Rα and its A10-mediated proteolytic release was analyzed by SDS-PAGE and immunoblotting using antibodies directed against the myc-tagged receptor, both in the presence and absence of Scube2. As expected, IL-2Rα release from $A10^{-/-}$ cells is severely impaired and its release from A10-expressing HEK control cells is not controlled by Scube2. **A')** Quantification of IL-2Rα release as shown in A. IL-2Rα release from HEK cells expressing Scube2 was set to 100%. One-way ANOVA, Dunnett's multiple comparison test. ns: p>0.05, ****: p<0.0001, n=8.

See Supplementary Figure 2 for loading controls and Supplementary Table 1 for detailed statistical information.

Scube2 EGF domains and the spacer domain increase Shh release

Which Scube2 domains mediate A10-mediated specific Shh release in serum-depleted media? To address this question, we co-expressed dual lipidated, PM-associated Shh together with Scube2 and two artificial Scube2 variants: Scube2ΔCUB, which lacks the C-terminal CRD and CUB domains, and Scube2ΔEGF, which lacks the nine N-terminal EGF domains (schematics of these proteins are shown in Figure 5A). We then compared their ability to enhance Shh solubilization by SDS-PAGE and immunoblotting under serum-depleted conditions, using the same experimental design as described above. The positive control Scube2 significantly enhanced A10-driven Shh solubilization (Figure 5B, B', Supplementary Figure 3A), confirming our previous observations. Notably, the EGF domains and spacer region of Scube2 (Scube2ΔCUB) enhanced Shh release, but to a lesser extent than Scube2 (Figure 5C, C', Supplementary Figure 3B), and Scube2ΔEGF, which lacks all nine EGF domains, no longer enhanced A10-driven Shh release (Figure 5D, D', Supplementary Figure 3C). These results suggest that the EGF domains strongly contribute to Scube2-enhanced Shh solubilization from the PM, at least when Shh is released from A10- and Disp-expressing HEK293 cells into serum-depleted media. Interestingly, a *Drosophila* ortholog of Wnt Inhibitory Factor (WIF) called Shifted (Shf), a soluble protein that helps modulate Hh distribution in the wing imaginal disc [61, 62], also contains five EGF-like repeats but no CUB domain and CRD, raising the possibility that it functions in a similar manner in the fly as the Scube2 EGF domains do in our cell-based assays.

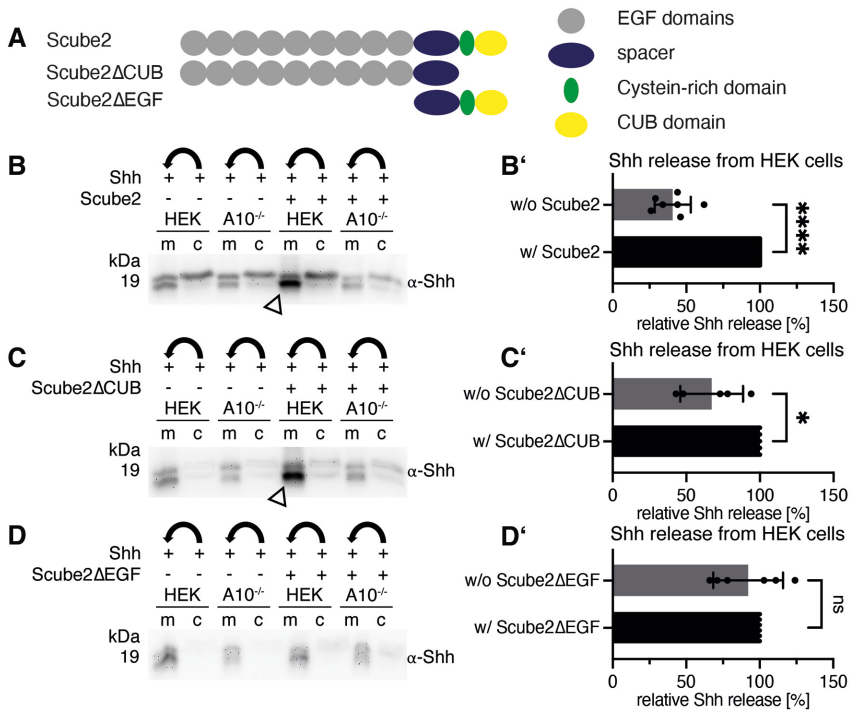

Figure 5: The EGF and spacer domains of Scube2, but not the CUB/CRD/spacer, increase A10-controlled Shh release. A) Schematic representation of the Scube2 variants used in this experiment. Full-length Scube2 consists of nine EGF domains, followed by a spacer region, a cysteine-rich domain and a CUB domain. Scube2ΔCUB consists of all nine EGF domains and the spacer region. Scube2ΔEGF consists only of the spacer domain, the CRD domain and the CUB domain. **B-D)** Shh release from HEK cells or A10$^{-/-}$ cells in the presence or absence of Scube2 or the Scube2 variants. Shh solubilization was analyzed by SDS-PAGE and immunoblotting. **B)** Full-length Scube2 specifically increases A10-mediated Shh solubilization from HEK cells. **C)** Scube2ΔCUB also increases Shh solubilization. **D)** Scube2ΔEGF does not increase Shh solubilization from HEK cells. **B'-D')** Quantification of Shh solubilization in the presence or absence of Scube2 or the Scube2 variants. Shh release from HEK293 cells in the presence of Scube2 or the respective Scube2 variants was set to 100%. Scube2 and Scube2ΔCUB strongly increase A10-driven Shh release, in contrast to Scube2ΔEGF, which is not active. Unpaired t-test, two-tailed. ****: $p<0.0001$, *: $p<0.05$, ns: $p>0.05$, n=7 (B'), n=5 (C'), n=6 (D'). See Supplementary Table 1 for detailed statistical information.

Scube2 binds multiple serum proteins

How can the activity of Scube2 EGF domains in regulating Shh release be mechanistically explained? In general, EGF domains in other proteins are involved in homophilic or heterophilic protein-protein interactions [28, 29], such as between the EGF domains of thrombomodulin and the protease thrombin [63], between the EGF domains of the low-density lipoprotein receptor (LDLR) and protein convertase subtilisin/kexin type 9 [64], or between low-density lipoprotein receptor-related protein 1 (LRP1) and apolipoprotein E and alpha-2-macroglobulin, the latter being an inhibitor of all four proteinase classes [65]. Therefore, we hypothesized that Scube2 activity in Shh release may also be based on Scube2 interactions

with proteases, protease regulators, or soluble Shh acceptors. To test this hypothesis, we expressed Scube2 in serum-containing medium, bound FLAG-tagged Scube2 to anti-FLAG-tagged Sepharose, and precipitated Scube2 and interacting proteins. Scube2 interactors were then identified by mass spectrometry using a bovine serum database [66] (Table 1). This approach identified 11 Scube2 bait peptides along with bovine alpha-1-antiprotease (6 peptides, sequence coverage 17.5%) and alpha-2-antiplasmin (2 peptides, sequence coverage 3.9%), both serine protease inhibitors. We also found that Scube2 binds to fetuin-B (4 peptides, sequence coverage 9.6%) and to alpha-2-macroglobulin (14 peptides, sequence coverage 9.7%), the protein that also binds LRP1. An interaction of plasminogen protease with Scube2 (4 peptides, 4.8% coverage) was also detected. We note that A10 was not detected because it is a membrane-associated protein and is not present in serum. Nevertheless, our results suggest that a potential role of Scube2 is to indirectly regulate Shh proteolysis at the cell surface through the recruitment of proteases and protease regulators, consistent with A10-controlled Shh release.

Another Scube2 interactor identified in our screen was apolipoprotein A1 (ApoA1, 3 peptides, 11.3% sequence coverage). ApoA1 is the non-mobile signature protein of high-density lipoproteins (HDL), which serve as established acceptors for peripheral free cholesterol. Importantly, HDL is present not only in the serum but also in the interstitial fluid [40, 67] that leaks from the blood capillaries and fills the spaces around peripheral cells in both the embryo and the adult. In this study, we focused on the interaction of Scube2 with HDL for three main reasons: First, Hh and Shh solubilization is known to require lipoprotein (LPP) carriers, including HDL, both *in vivo* and *in vitro* [40, 46]. The second reason, which is related to the first, is that we have previously rediscovered that Disp-dependent Shh release is strictly dependent on the presence of HDL in the medium. This is because Shh release is blocked in media completely devoid of HDL, even if Disp, A10 and Scube2 are present [41]. The third reason is that we have previously observed that increasing HDL levels in media enhance Disp-mediated Shh solubilization in an increasingly Scube2-independent manner [41]. Taken together, these results suggest that Scube2/HDL interactions contribute to Disp- and A10-mediated Shh release.

Protein ID	Protein names	detected Peptides	Coverage [%]	MS/MS count	function
Q9NQ36	Scube2	11	13.7	13	bait
Q7SIH1	α2-macroglobulin	14	9.7	13	inhibitor of all four proteinase classes
Q2UVX4	Complement C3	11	6.2	10	protease with CUB domain
P34955	α1-antiproteinase	6	17.5	26	proteinase inhibitor
Q58D62	Fetuin-B	4	9.6	7	protease inhibitor
P06868	Plasminogen	4	4.8	3	protease
P15497	Apolipoprotein A1	3	11.3	3	HDL constituent
P28800	α2-antiplasmin	2	3.9	5	serine protease inhibitor

Table 1: Scube2 interacting serum proteins, as determined by Scube2 immunoprecipitation and mass spectrometric analysis of the top 7 associated proteins. Albumin was the most prominent hit, but was considered a contaminant due to its very high serum abundance and is therefore not listed.

Scube2 control of Shh release becomes increasingly dispensable as extracellular HDL levels rise

To test the physical interaction between Scube2 and HDL in more detail, we expressed Scube2, Scube2ΔEGF lacking all nine EGF domains, and Scube2ΔCUB, bound the FLAG-tagged proteins to anti-FLAG-tagged Sepharose, precipitated Scube2 and Scube2 variants together with interacting serum proteins as described above, and analyzed the precipitate by SDS-PAGE and immunoblotting (Figure 6A). ApoA1 was enriched in Scube2 and Scube2ΔCUB precipitates, but not when Scube2ΔEGF, which lacks the EGF domains, was analyzed. These results show that the EGF domains of Scube2 bind HDL, possibly to facilitate Disp- and A10 mediated Shh transfer to the soluble carrier. To directly test such a facilitating function of Scube2 in Shh transfer to HDL, we solubilized Shh from HEK cells and $A10^{-/-}$ cells in serum-free media at high (40 µg/mL) extracellular HDL levels and in the presence or absence of Scube2. Of note, in this set of experiments, cells were repeatedly washed to remove all traces of serum before serum-free or HDL-reconstituted serum-free media were added and Shh release was monitored. As shown in Figure 6B and Supplementary Figure 4A, Shh release in the HDL-containing medium remained largely A10-dependent (Figure 6B'), but Shh release from A10-expressing cells was rendered completely independent of Scube2 (Figure 6B''). This confirmed our published observation that Scube2 enhances Disp-mediated Shh solubilization under conditions where serum or HDL levels are low, and that high HDL levels render Scube2 function dispensable [41]. These data are also consistent with the results showing that the EGF domains are required for Scube2-enhanced Shh release (Figure 5). In addition, the majority of solubilized proteins were N-truncated (Figure 6B, arrowhead, Supplementary Figure 4A) and lacked the N-terminal palmitate (Figure 6C, the soluble HDL-associated protein elutes in fractions #33-35, note that only a small fraction of dually processed soluble protein is detected in fraction #29, dual-lipidated control R&D Shh elutes in fraction #37), consistent with the involvement of A10 in Shh release. However, unlike Shh released under serum-depleted conditions, HDL-released Shh is not C-terminally processed, suggesting that the Shh cholesterol moiety serves to associate Shh with the soluble carrier and that HDL association protects the C-peptide from A10 cleavage. We note that the HDL-associated N-truncated ligand is highly bioactive (Supplementary Figure 4 B-D, see also [41] for a thorough characterization of the HDL-associated Shh biofunction), indicating the physiological relevance of Disp- and A10-mediated Shh transfer to HDL carriers. Importantly, this is also true in the absence of Scube2, suggesting that Scube2 does not directly contribute to Shh/HDL signaling in target cells (Supplementary Figure 4 B,C). Again, A10-independent solubilization of artificially monolipidated Shh variants ^{C25A}Shh and ShhN (Supplementary Figure 4 E,F) confirmed that A10-controlled Shh transfer to HDL acceptors is strictly dependent on dual Shh lipidation.

Next, we characterized the Scube2 dependence of Shh solubilization at increasing HDL concentrations up to 40 µg/mL in detail. As previously observed in Disp-expressing HEK293 control cells [41], Shh solubilization became less Scube2 dependent with increasing amounts of HDL in serum-free media (Figure 6D, Supplementary Figure 5A). This suggests that Scube2 is only required when extracellular HDL availability is low, and we confirmed this finding in our A10 expressing cells: Scube2 increased Shh truncation and release at 10µg/ml HDL in the medium, whereas HDL concentrations above 20µg/ml rendered Shh release completely independent of Scube2. This result is consistent with the above finding that 40 µg/ml HDL

consistently renders Shh release Scube2 independent. We made a similar observation when Scube2ΔCUB was used instead of Scube2 (Figure 6E, Supplementary Figure 5B): Shh solubilization again became progressively less dependent on Scube2ΔCUB as HDL concentrations in the media were increased. Shh solubilization was significantly enhanced up to 20 µg/ml HDL in the medium, but 30 µg/ml or more released high levels of Shh in a Scube2ΔCUB-independent manner. The similar activity of Scube2 and Scube2ΔCUB in this experimental setup supports our previous results showing that Scube2ΔCUB enhances Shh solubilization to almost the same extent as full-length Scube2 under serum-depleted conditions (where HDL levels are also low, Figure 5) and that ApoA1 was not co-IPed when Scube2ΔEGF was used as bait (Figure 6A). This form was also inactive at low HDL concentrations in our release assays (Supplementary Figure 5C). Taken together, our results support that Scube2 binds soluble HDL via its EGF domains to facilitate Disp-mediated and A10-controlled Shh release. We note that all nine EGF domains of Scube2 share high sequence identity with the EGF domains of the seven members of the structurally related LDL receptor family (Table 2). This family includes LDLR, VLDLR, LDLR related protein 1 (LRP1), LRP1b, LRP2/megalin, LRP4 and LRP8/apoE receptor-2 [68]. While LDLR and VLDLR bind and endocytose apoB- and apoE-containing lipoproteins, respectively, LRP1 is a ubiquitously expressed 600-kDa endocytic receptor responsible for cellular uptake and plasma clearance of more than 30 macromolecules including apolipoprotein E-containing LPPs [69] and protease-protease inhibitor complexes [70]. LRP2/megalin is an endocytic receptor that also binds and internalizes more than 75 putative ligands, including protease-protease inhibitor complexes, LPPs and, interestingly, Shh [71]. These shared multiligand binding properties between Scube2 (Table 1) and the LDL receptor family, particularly with proteases and protease inhibitors, but also with LPPs, suggest not only structural similarities between the two families of molecules, but also functional similarities. A notable difference between Scube2 and the LDL receptor family is that ligand binding to the latter results in their internalization, whereas Scube2 is a soluble molecule and acts in the opposite direction to release ligands from the cell.

	LDLR	**LRP1**	**LRP2**	**LRP4**	**LRP5**	**LRP6**	**LRP8**
EGF1	50.00 %	35.29 %	39.39 %	35.29 %	32.26 %	30.00 %	31.43 %
EGF2	52.00 %	38.71 %	42.86 %	46.88 %	43.75 %	50.00 %	48.00 %
EGF3	55.17 %	41.67 %	41.67 %	44.44 %	44.74 %	41.67 %	52.78 %
EGF4	37.14 %	37.84 %	37.84 %	35.14 %	35.14 %	40.54 %	40.54 %
EGF5	38.24 %	46.67 %	50.00 %	38.89 %	54.17 %	33.33 %	41.67 %
EGF6	51.72 %	51.53 %	47.22 %	47.22 %	47.22 %	50.00 %	55.56 %
EGF7	35.29 %	48.39 %	45.16 %	44.44 %	47.22 %	41.67 %	47.22 %
EGF8	35.71 %	46.43 %	35.29 %	45.83 %	40.91 %	40.91 %	33.33 %
EGF9	48.28 %	45.19 %	43.33 %	44.44 %	36.11 %	42.11 %	40.00 %
combined	42.50 %	22.11 %	43.02 %	42.50 %	44.74 %	44.44 %	42.11 %

Table 2: Scube2 EGF domains show high sequence identity with the EGF consensus sequences of the LDLR and the LRPs. This indicates similar functions of Scube2 EGF-domains and the EGF-domains of the LDLR and of LRP1-6.

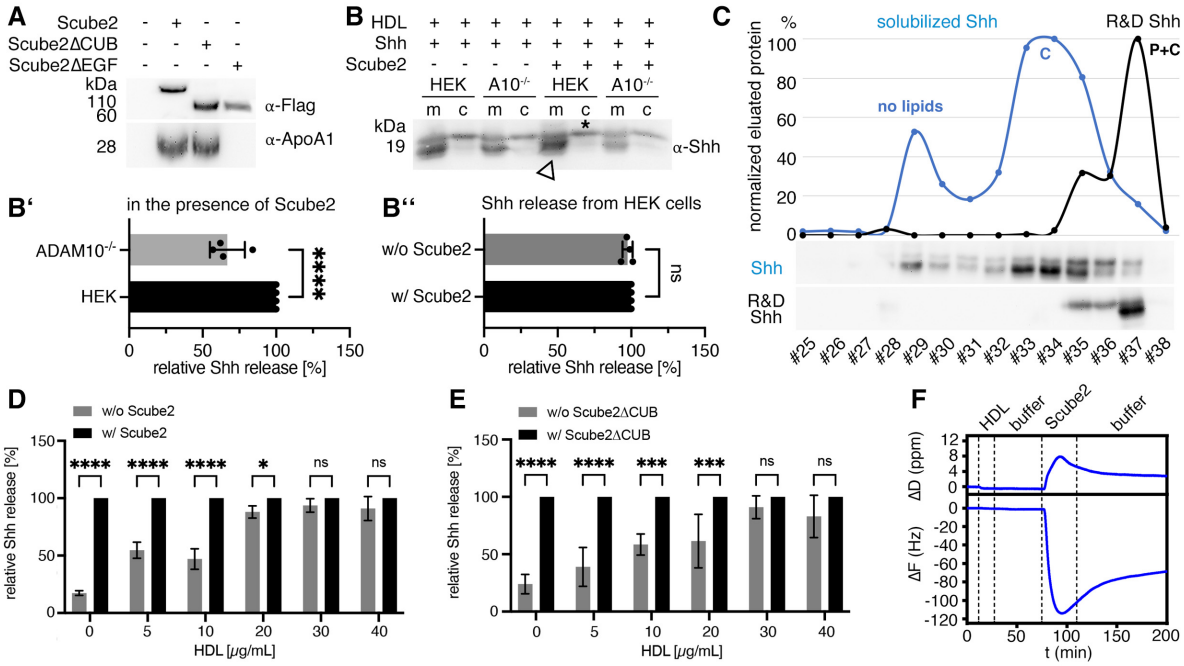

Figure 6: Scube2 and a minimal EGF domain/spacer construct increase Shh solubilization under conditions of low HDL concentration via HDL recruitment to HS. A) HDL co-immunoprecipitates with the Scube2 bait and also with the Scube2ΔCUB bait, but not with Scube2ΔEGF. **B)** 40µg/ml purified human HDL in serum-free media solubilized Shh from cells that were repeatedly washed to remove all traces of serum before the experiment. Levels of Shh solubilization from HEK cells and A10$^{-/-}$ cells in the presence or absence of Scube2 were analyzed by SDS-PAGE and immunoblotting as described previously. Soluble truncated Shh is indicated by an arrowhead. **B')** Quantification of Shh solubilization from HEK cells or A10$^{-/-}$ cells, both in the presence of Scube2. Shh release from HEK cells was set to 100%. Unpaired t-test, two-tailed. ****: p<0.0001, n=4 independent release assays. **B'')** Quantification of Shh solubilization from HEK control cells in the presence or absence of Scube2. HEK cells expressing Scube2 were set to 100%. Unpaired t-test, two-tailed. ns: p>0.05. n=4 independent release assays. **C)** RP-HPLC confirmed the loss of the N-terminal palmitoylated Shh peptide during Disp-, A10- and Scube2-regulated solubilization and showed that only the C-terminal cholesterol (C), but not the palmitate (P), associates the N-processed Shh molecule with HDL [41]. **D)** Shh solubilization in medium containing increasing concentrations of HDL in the presence or absence of Scube2. HDL concentrations in media and Scube2 contribution to Shh solubilization are inversely correlated. ****: p<0.0001, *: p<0.05, ns: p>0.05, n=3. **E)** Scube2ΔCUB and Scube2 have similar Shh release-enhancing activity profiles at low HDL levels. Two-way ANOVA. ****: p<0.0001, ***: p<0.001, ns: p>0.05, n=3. **F)** Scube2, but not 80 µg/ml HDL, binds to an HS-functionalized artificial PM, as indicated by a decrease in *F* and an increase in *D* during Scube2 binding in QCM-D measurements, but only a small increase in *D* and no change in *F* when HDL was applied to the sensor surface. See Supplementary Figure 6 for detailed information on the QCM-D technique.

HS recruits Scube2, but not isolated HDL, to an artificial cell surface

Previous work has shown that Scube2 activity requires specific HS expression on the surface of Shh source cells and that clustered basic amino acids in the Scube2 spacer domain associate the soluble molecule with heparin and cellular HS [13, 16]. The physiological

relevance of unimpaired Scube2/HS interactions at the cell surface of Shh expressing cells was supported by blockade of Scube2-enhanced Shh solubilization by soluble heparin, which decreases Scube2 binding to the cell surface, and by sodium chlorate, an inhibitor of cell surface HS sulfation. Fluorescence activated cell sorting (FACS) confirms these published findings and shows that removal of cellular HS by treatment with heparinases or deletion of the HS-binding spacer region of Scube2 strongly reduces its ability to bind to cell surfaces (Supplementary Figure 6A-C). In notable contrast, soluble HDL does not bind to HS or heparin [72], and therefore does not readily associate with HS-rich Shh release sites on the cell surface. Based on these considerations, we hypothesized that soluble Scube2/HDL complexes could bind to cell surface HS, thereby bridging the gap between HS-associated Shh substrates and their soluble HDL acceptors. We tested this hypothesis by measuring HDL and Scube2 interactions with a reconstituted artificial PM using quartz crystal microbalance with dissipation monitoring (QCM-D) technology. The core of the QCM technology is an oscillating quartz crystal sensor disc with a resonance frequency related to the mass of the disc. This allows real-time detection of nanoscale mass changes on the sensor surface by monitoring changes in the resonance frequency (ΔF): adsorption of molecules on the surface decreases F, while a mass decrease increases F. QCM-D measures an additional parameter, the change in energy dissipation D, where ΔD correlates with layer softness, which tends to increase as mass is added to the sensor surface. As shown in Figure 6F and Supplementary Figure 6D,E, incubation of the QCM-D chip with HDL did not induce a shift in F and only slightly changed D, confirming that HDL does not bind highly sulfated forms of HS. In contrast, Scube2 induced a strong shift in the resonance frequency ($-\Delta F$) of about -90 Hz, indicating effective binding, and a proportionally increased energy dissipation (ΔD) of the heparin/Scube2 film. Both parameters reversed somewhat after washing buffer injection into the QCM-D chambers, indicating limited Scube2 washout from heparin. These results demonstrate the ability of HDL-associated Scube2 to recruit the carrier to HS-rich cell surface sites to which HDL would not otherwise bind. This increases the local concentration of HDL at these sites, which in turn accelerates Disp-mediated transfer of the cholesteroylated Shh C-terminus to HDL acceptors and final processing of the N-terminal peptide anchor to complete Shh release. We propose that artificially high HDL concentrations in the media, as achieved in our in vitro experiments, render Scube2 recruitment of HDL less critical due to the law of mass action, which states that the rate of a reaction (here Disp- and A10-mediated Hh transfer to HDL) is directly proportional to the concentrations of the reactants.

Discussion:

Cell surface Hh release sites consist of large, light microscopically visible Hh clusters (which also form on the surface of HEK293 (Figure 7A,B), supporting the physiological relevance of our experimental system), and it is well established that Disp and Scube2 release Shh from these sites. Consistent with this, HEK293 cells lacking Disp or Scube2 function fail to solubilize Shh [34, 35, 73], and we recently rediscovered that HDL accepts Shh from Disp at these release sites [41]. These results are consistent with the established synergistic activity of Disp and Scube2 in Shh release [21, 22] and with serum LPPs acting as soluble Hh carriers *in vitro* and *in vivo* [40, 46]. Here we report that A10 also contributes to Shh solubilization *in vitro*, as Shh release from HEK293 cells expressing Disp but lacking A10 and from HEK293 cells expressing A10 but lacking Disp is impaired to a similar extent. We further supported the *in vivo* relevance of A10-regulated Shh shedding by tissue-restricted expression of a dominant-negative

form of the *Drosophila* A10 ortholog, Kuz^{DN}, in the developing eye disc. The resulting suppression of endogenous Kuz activity in the developing eye delayed furrow progression by endogenous Hh, as predicted by our model, to a degree similar to that of homozygous hh^{bar3} eye discs, which carry an eye disc-specific Hh promoter mutation and therefore express very little Hh to move the furrow [74, 75], and exceeding that caused by large homozygous cell clones that lack most Disp function. These results show that not only Disp and Scube2 (and HDL) are required for Shh release, but that A10/Kuz is also essential to control a final step in morphogen release: only cells in which all four factors are present solubilize Shh to the maximum extent. Since most solubilized Shh lacked the N-palmitate but retained the C-cholesterol moiety (Figure 6C) [41], we propose that the role of A10 is to specifically cleave the N-terminal palmitoylated membrane anchor while Disp transfers the cholesteroylated C-terminal Shh peptide from the cell surface to LPP acceptors (Figure 7C-E). Importantly, in contrast to previous descriptions of processed or depalmitoylated recombinant Hhs with reduced biofunction [6, 76], we show that the HDL-associated N-truncated Shh variant is highly bioactive, suggesting that HDL may not only function in Hh transport but also contribute to Ptc receptor binding and signaling.

Our Disp- and A10-controlled Shh release model raises the important question of how to mechanistically explain the established role of Scube2 in facilitating Shh release and signaling if it is not the acceptor and transporter for Shh. One possible answer comes from our previous observation that the addition of high levels of purified HDL to serum-free media of Shh-expressing HEK293 cells renders Disp-mediated Shh release Scube2 independent [41] (Figure 7D). We confirm here that Scube2 specifically enhances Shh release at low HDL concentrations in the media and that Shh release becomes less Scube2 dependent as HDL levels in the media increase (Figures 6D,E). This led us to hypothesize that Scube2 facilitates Shh transfer to HDL in specific tissues or developmental contexts *in vivo* or at low HDL levels in media *in vitro*, possibly by binding and recruiting HDL to and enriching it at the punctate HS-rich cell surface sites of Shh release (Figure 7E).

Indeed, the assembly of punctate Hh release sites (Figure 7A,B) is known to be driven by direct interactions of two positively charged polybasic motifs present on all Hhs [77, 78] with highly negatively charged cell surface HS [7, 13]. Scube1 and Scube2 also bind cell surface HS via polybasic motifs located in their spacer domains [16, 32]. Thus, the role of HS is to assemble large Hh ligand complexes at the cell surface (Figure 7A,B) and to also recruit soluble release factors such as Scube2 to these sites (Figure 7E) [16]. In contrast, the required HDL acceptor for Shh is the only known LPP that does not strongly bind HS/heparin [72], unlike the other major LPPs VLDL, LDL, and chylomicrons [79], and therefore would not readily associate with HS-rich Shh release sites (this property is exploited in clinical analyses of blood cholesterol where the non-HDL fraction is precipitated with heparin and the remaining soluble HDL is measured [80]). We hypothesized that the inability of HDL to bind cell surface HS by itself might be compensated by Scube2 binding to HDL and cell surface HSPGs [16], thereby enriching HDL at the spatially defined cell surface Shh release complex (Figure 7E). In this study, we supported this hypothesis by mass spectrometry demonstrating Scube2 interactions with ApoA1, the characteristic immobile protein component of HDL. Scube2 pull-down of HDL from serum confirmed this result and showed that HDL associates with the N-terminal EGF domains of Scube2, which interestingly share extensive sequence identity with the EGF domains of LPP receptors and the multi-ligand/ApoE-binding low-density LPP receptor-related proteins (LRPs, Table 2). Consistent with this, EGF- and HS-binding spacer domains of Scube2 are sufficient to

strongly enhance Shh release under serum-depleted (i.e., low HDL) conditions (Figure 5C, 6D). Finally, we supported our hypothesis of Scube2-dependent HDL recruitment to HS by QCM-D. Taken together, our results show that soluble HDL binds to the EGF domains of Scube2 and the spacer domain binds to cell surface HS [16], thereby concentrating HDL on HS-rich cell surface clusters to which it would not otherwise bind [13], and possibly making HDL association more robust. This step completes the assembly of the Shh release complex, allowing A10 to cleave a Shh anchor from the PM and Disp to transfer the cholesteroylated protein product to the HDL (Figure 7E).

Our results showing that Scube2 recruitment of HDL acceptors merely facilitates and enhances Shh release under conditions of low HDL abundance – as opposed to being an essential Shh carrier itself [21, 22] – are supported by targeted Scube2 knockouts in mice and zebrafish, which result in relatively mild and tissue-restricted developmental defects [17, 81]. Our results are also consistent with the fact that *Drosophila melanogaster* does not express a Scube2 ortholog, despite the otherwise high conservation of the Hh release machinery in the fly. In particular, LPPs – known as lipophorins in insects – have been shown to play an essential role in Hh release and transport *in vivo* [40, 46]. One possibility to explain the lack of Scube orthologs in *Drosophila,* despite the established role of LPPs in Hh release and transport, is that insects have an open circulatory system, both in larvae and adults. Here, the hemocoel directly bathes developing cells with oxygen, nutrients, and high levels of lipophorins without distinguishing between "blood" and "interstitial fluid". Therefore, lipophorin concentrations in the hemocoel may be high enough to readily act as effective Hh acceptors, similar to the "high HDL" conditions used in our cell culture experiments that rendered Scube2 function unnecessary. Another difference between vertebrate and insect LPPs is that lipophorin, unlike HDL, binds HS on the cell surface [82] and therefore does not require a facilitator protein to accept Hh from Disp-expressing cells. A final possibility to explain the lack of a Scube ortholog in insects is that the soluble HS-binding protein Shifted (which carries five EGF-like domains) may perform this function instead [62].

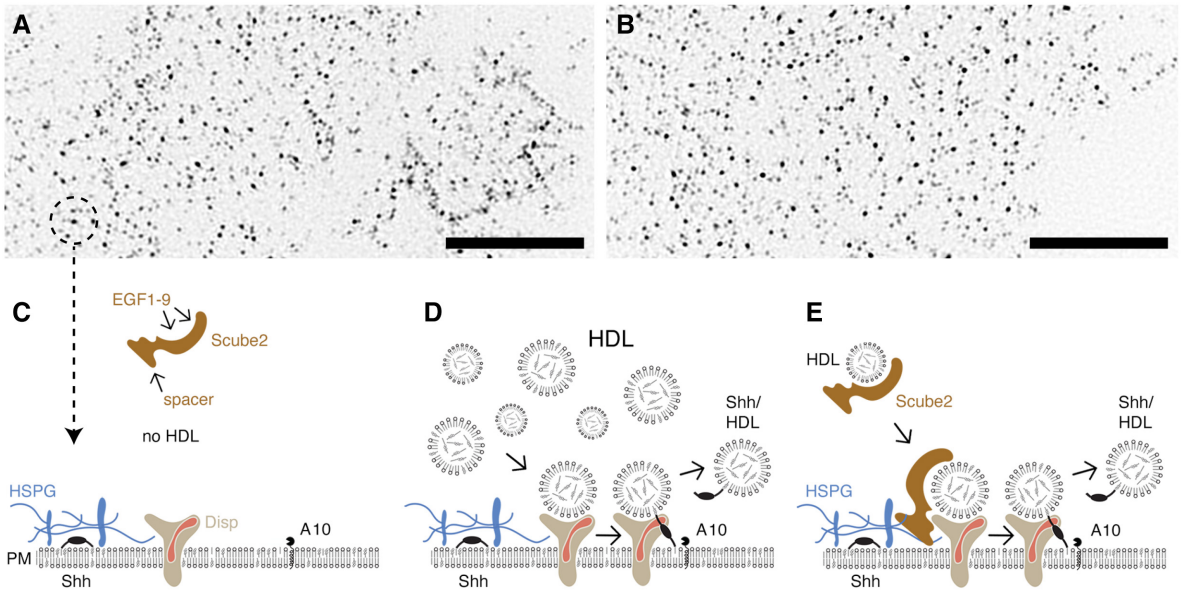

Figure 7: Model of Disp-mediated Shh transfer to HDL. We propose that Disp-mediated Shh solubilization requires HDL and A10, whereas the requirement for Scube2 is relative and depends on the amount of available HDL carriers. **A,B)** TIRF-SIM of Shh-transfected HEK293 cells (A) or Disp$^{-/-}$ cells (B) using the monoclonal anti-Shh antibody 5E1 shows unchanged cell surface clustering of overexpressed Shh in both cell lines. Scale bar: 10 µm. **C)** Dual-lipidated Shh colocalizes with HSPGs [7] (left). The availability of HDL carriers at the cell surface is a critical step for Shh release: In the absence of HDL, the Disp-regulated release complex is incomplete and Shh cannot be released, even in the presence of Scube2 [41]. EGF domains and the HS-binding spacer region are indicated. **D)** High HDL levels, as modeled in our experiments, result in frequent random encounters of HDL with the Shh release complex based on the law of mass action. This allows Disp to more effectively transfer the C-terminal Shh cholesterol moieties to HDL. This first step of partial Shh extraction exposes the N-terminal cleavage site for subsequent proteolytic processing by A10. Both activities release Shh from the PM. **E)** We propose that one role of Scube2 is to increase the frequency of HDL encounters with the release complex when HDL levels are low. This may be achieved by recruiting the soluble HDL/Scube2 complex to the punctate Shh/HSPG clusters at the cell surface [7, 13, 16]. This model explains why Scube2-regulated Shh solubilization is best achieved under serum-depleted conditions: We propose that Scube2, which has captured HDL and recruited it to the cell surface, forms a HS-associated Scube2/HDL reservoir that allows Shh solubilization to continue even after the medium is changed to serum-free DMEM. In contrast, careful prior washing of cells depletes the Scube2/HDL reservoir, thereby minimizing Shh release [41]. See Discussion for details.

Acknowledgments

The excellent work of Petra Jakobs, Sabine Kupich and Reiner Schulz is gratefully acknowledged. **Funding:** This work was funded by the Deutsche Forschungsgemeinschaft (DFG, German Research Foundation) – Project-ID 386797833 – SFB 1348: Dynamic Cellular Interphases to K.G and S.V.W., and GR1748/9-1 to K.G. We thank the CECAD Proteomics

Facility for the analysis of proteome data. This work was supported by the large instrument grant INST 216/1163-1 FUGG by the German Research Foundation (DFG Großgeräteantrag).

Competing interests: Authors declare no competing interests.

Materials and Methods

Fly lines: The following fly lines were used: GMR-GAL4 (GMR>): GMR17G12 (GMR45433-GAL4): P(y[+t7.7]w[+mC]=GMR17G12-GAL4)*attP2*, Bloomington stock #45433 (discontinued but available from our lab), and w; P(w[+mC]=UAS-kuz.DN)2, Bloomington stock #6578. We used an established protocol [78] that was adapted to delete disp function from large clones in the eye disc. In brief, the hsFLP in flies carrying a disp hypomorphic disp^{S037707} allele [34] flanked by an FRT site (P(ry[+t7.2]=hsFLP)12,y[1]w[*];P(ry[+t7.2]=neoFRT)82B;P(w[+mC]=lacW)disp[S037707]/TM6B,Tb[1], Bloomington stock #53711) was replaced with eye disc specific eyFlp3.5 and an Rps3 allele, generating flies with the genotype eyFlp3.5/+;FRT82 P(w[+mC]=lacW)disp[S037707]/ FRT82 Rps3 UbiGFP. Kuz^{DN} transgene expression in the morphogenetic furrow of the eye disc was conducted by crossing both lines at 25°C. Ommatidia number of the resulting *UAS-Kuz^{DN}/GMR-GAL4* flies were analyzed with a Nikon SMZ25 microscope. *white^{1118}* flies served as positive controls and *+/+;hh^{bar3}/hh^{bar3}* flies served as negative controls.

Cell lines. The generation and validation of Disp knockout cells (Disp$^{-/-}$) and HEK control cells was previously described [33]. To specify the ADAM target regions for the CRISPR/Cas9-mediated genome editing, the third exon of the human A10 genomic sequence (ENST00000260408) and the first exon of the human ADAM17 genomic sequence (ENST00000310823) were submitted to an online CRISPR Design Tool (http://tools.genome-engineering.org). For each targeted gene, a pair of oligonucleotides (A10g#2_F: 5'ACCGATACCTCTCATATTTACAC, A10g#2_R: 5'AACGTGTAAATATGAGAGGTATC; A17g#2_F: 5'ACCGCCGCGACCTCCGGATGACC, A17g#2_R: 5'AACGGTCATCCGGAGGTCGCGGC) was annealed, phosphorylated and subsequently cloned into the SapI-digested guideRNA expressing plasmid LeGO-Cas9-iC-puro+cgRNA_SapI (generously provided by Boris Fehse, UKE Hamburg). The resulting plasmids were designated LeGO-Cas9-A10 and LeGO-Cas9-ADAM17, respectively. Genome-editing to achieve protease-deficient HEK293 cells – CRISPR/Cas9 plasmids were transfected into HEK293T cells using TurboFect Transfection Reagent (Life Technologies, Carlsbad, CA). 48 h following transfection, cells were grown in the presence of 1 µg/ml puromycin for additional 48 h to enrich successfully transfected cells. For the isolation of genome-edited cells, cell populations were subjected to FACS (fluorescence activated cell sorting) analysis after immunostaining with PE anti-human CD156c antibody (BioLegend, San Diego, CA) and A300E antibody (Institute of Biochemistry, Kiel, Germany) and single-cell sorted into 96-well plates. Single cell clones were further expanded and the efficient knock-out of A10 and A17 confirmed via FACS and Western blotting. Complete A10 knock-out was finally confirmed by sequencing. Importantly, Disp and

A10/A17 were deleted in HEK293 cells or the HEK293 cell derivative Bosc23, which makes our results comparable to earlier assys that were conducted in this cell type [21, 22]. Disp$^{-/-}$, HEK, A10$^{-/-}$ and A17$^{-/-}$ cells, and C3H10T1/2 reporter cells were maintained in DMEM supplemented with 10% FCS and 100 µg/mL penicillin-streptomycin. Sequencing of A10$^{-/-}$ cells revealed deletions in 3 different A10 loci, consistent with the modal chromosome number of 64 in HEK293 cell lines (https://www.phe-culturecollections.org.uk/products/celllines/) that introduced stop codons at or upstream of codon#110 in the inhibitory N-terminal propeptide sequence.

Cloning of recombinant proteins. Shh expression constructs were generated from murine cDNA (NM_009170: nucleotides 1-1314, corresponding to amino acids 1-438; and ShhN: nucleotides 1-594, corresponding to amino acids 1-198) and human Hhat cDNA (NM_018194). Both cDNAs were cloned into pIRES (Clontech) for their coupled expression from bicistronic mRNA to achieve near-quantitative Shh palmitoylation [23]. ShhN (nucleotides 1-594, corresponding to amino acids 1-198) and Hhat were also cloned into pIRES. ^{C25S}Shh was generated by site-directed mutagenesis (Stratagene). Unlipidated ^{C25S}ShhN cDNA and non-palmitoylated ^{C25S}Shh cDNA (amino acids 1-438) were inserted into pcDNA3.1 (Invitrogen). Primer sequences can be provided upon request. cDNAs encoding IL-2Rα and IL-6Rα were provided by the Garbers lab. Human Scube2 constructs were a kind gift from Ruey-Bing Yang (Academia Sinica, Taiwan). Where indicated, dual-lipidated, HEK293-derived human Shh (R&D Systems, 8908-SH) served as a bioactivity control and to quantify Bosc23-expressed, TCA-precipitated proteins on the same blots.

Protein detection. HEK cells, Disp$^{-/-}$ cells and A10$^{-/-}$ cells were seeded into six-well plates and transfected with 1 µg Shh constructs together with 0.5 µg Scube2 or empty cDNA3.1 by using Polyfect (Qiagen). Cells were grown for 2 days at 37°C with 5% CO_2 in DMEM containing 10% FCS and penicillin-streptomycin (100 µg/mL). Serum-containing media were aspirated and serum-free DMEM added for 6 h, harvested, and centrifuged at 300*g* for 10 min to remove debris. Supernatants were incubated with 10% trichloroacetic acid (TCA) for 30 min on ice, followed by centrifugation at 13,000*g* for 20 min to precipitate the proteins. Cell lysates and corresponding supernatants were analyzed on the same reducing SDS polyacrylamide gel and detected by Western blot analysis by using rabbit-α-Shh antibodies (Cell signaling C9C5), rabbit-α-GAPDH antibodies (Cell Signaling, GAPDH 14C10, #2118), or anti-β-actin antibodies (Sigma-Aldrich, A3854) followed by incubation with horseradish peroxidase-conjugated secondary antibodies. FLAG-tagged Scube2 was detected by using polyclonal α-FLAG antibodies (Sigma, St. Louis, USA). GAPDH, β-actin (for cell lysates), or Ponceau S (for media) served as a loading control. Note that the amounts of immunoblotted soluble and cellular Shh do not correlate inversely. This is because medium lanes represent all TCA-precipitated proteins or all proteins captured by heparin-pulldown in medium, while cells were directly lysed in SDS buffer and only a small fraction (about 5%) were applied to the gel. As a consequence, a 100% increase in Shh solubilization will correlate to only 5% reduction in the amount of cell-surface-associated Shh, and *vice versa*. Shh release was quantified by ImageJ and calculated as the ratio of total (cellular Shh or non-processed ^{C25S}ShhN) or processed (truncated) soluble Shh relative to the cellular Shh material. Relative Shh release from control cells (HEK) was set to 100% and

Shh release from Disp$^{-/-}$ or A10$^{-/-}$ cells was expressed relative to that value. This protocol was varied in three ways: For *serum-free* release, cells cultured in DMEM+10% FCS were carefully washed three times with serum-free DMEM before serum-free media were added for 6 h of protein release. For Shh release into *serum-depleted* medium, cells were not washed before the serum-free DMEM was added. For release into *HDL-containing* media, cells cultured in DMEM+10% FCS were carefully washed three times with serum-free DMEM before serum-free media supplemented with 40 µg/mL HDL were added for 12 h of protein release. For large-scale expression of Scube2, HEK293 cells were grown to 80-90% confluence in 15cm dishes and the medium was replaced with 16.6 ml DMEM containing 10% FCS. A premix consisting of 18.4 µg Scube2 and 276 µl polyethyleneimine (PEI) from stock (1mg/mL in H_2O, pH 7.0) in 920 µl medium without growth factors, serum, antibiotics or other proteins was incubated for 8 minutes. The premix was then supplemented with 8.3 mL DMEM containing 10% serum and added dropwise to the dish. The cells were incubated at 37°C. 8 hours after transfection, the medium was replaced with fresh DMEM containing serum and antibiotics and incubated for a further 24 hours. The medium was then aspirated, the cells were washed three times in DMEM without serum or antibiotics, and Scube2 was secreted into 20 mL of DMEM without serum or antibiotics for 24 hours. The supernatants were then transferred to 50ml Falcon tubes, centrifuged for 10 min at 14,000 rpm and the clarified media concentrated by Amicon ultrafiltration using membranes with a 30 kDa cut-off. Scube2 in the concentrates was quantified by SDS-PAGE prior to use in subsequent QCM-D experiments.

TIRF-SIM: nt-Ctrl and Disp$^{-/-}$ cells were seeded on gelatin-coated glass slides and transfected with Shh. Fixation was performed in 4% paraformaldehyde (PFA) and 2% glutaraldehyde for 10 min at room temperature, cells were washed 3 times with PBS and blocked with 5% goat serum in PBS for 1h. Cells were then incubated overnight with anti-Shh antibody (5E1 mouse, 1:250, DSHB, overnight) in blocking buffer at 4°C. The next day, cells were washed and incubated with FITC-labelled anti-mouse secondary antibody (1:300, Invitrogen) for 2h at room temperature. Analysis was performed on an LSM Airyscan detector using a 63x objective, with data deconvolved using Huygens Professional X11. Maximum intensity projections were generated using Fiji.

Shh bioactivity assay. Shh-conditioned HDL-containing DMEM was sterile filtered, FCS was added to the fractions at 10% and mixed 1:1 or 1:2 with DMEM supplemented with 10% FCS and 100 µg/mL antibiotics, and the mixture was added to C3H10 T1/2 cells. Cells were harvested 5 days after osteoblast differentiation was induced and lysed in 1% Triton X-100 in PBS, and osteoblast-specific alkaline phosphatase activity was measured at 405 nm by using 120 mM p-nitrophenolphosphate (Sigma) in 0.1 M Tris buffer (pH 8.5). Values measured in mock-treated C3H10 T1/2 cells served as negative controls.

Quantitative PCR (qPCR): Alternatively, C3H10T1/2 cells were stimulated with recombinant Shh/HDL with or without Scube2 in triplicate for 2 days. TriZol reagent (Invitrogen) was used for RNA extraction from C3H10T1/2 cells. A first strand DNA synthesis kit and random primers (Thermo, Schwerte, Germany) were used for cDNA synthesis before performing a control PCR with murine β-actin primers. Amplification with Rotor-Gene SYBR-

Green on a BioRad CFX 384 machine was conducted in triplicate according to the manufacturer's protocol by using the following primer sequences: actin forward: 5'CTATTGGCAACGAGCGGTTC, actin reverse: 5'CGGATGTCAACGTCACACTTC, Ptch1 forward: 5'GGGCTACGACTATGTCTCTC, Ptch1 reverse: 5'CTTTGATGAACCACCTCCAC, Gli1 forward: 5'CCCTGGTGGCTTTCATCAAC and Gli1 reverse: 5'TGACTCATCTGAGGTGGGAATC. Cq values of technical triplicates were averaged, the difference to β-actin mRNA levels calculated by using the ΔΔCt method, and the results expressed as log2-fold change if compared with the internal control of C3H10T1/2 cells stimulated with mock-transfected HDL-containing media.

Reverse-phase high performance liquid chromatography (RP-HPLC). HEK293 cells were transfected with expression plasmids for dual-lipidated Shh, unlipidated ^{C25A}ShhN control protein, cholesteroylated (non-palmitoylated) ^{C25A}Shh, and palmitoylated ShhN. Two days after transfection, cells were lysed in radioimmunoprecipitation assay buffer containing complete protease inhibitor cocktail (Roche, Basel, Switzerland) on ice and ultracentrifuged, and the soluble whole-cell extract was acetone precipitated. Protein precipitates were resuspended in 35 µL of (1,1,1,3,3,3) hexafluoro-2-propanol and solubilized with 70 µL of 70% formic acid, followed by sonication. RP-HPLC was performed on a C4-300 column (Tosoh, Tokyo, Japan) and an Äkta Basic P900 Protein Purifier. To elute the samples, we used a 0%-70% acetonitrile/water gradient with 0.1% trifluoroacetic acid at room temperature for 30 min. Eluted samples were vacuum dried, resolubilized in reducing sample buffer, and analyzed by SDS-PAGE and immunoblotting. Proteins expressed into the media were analyzed in the same way. Signals were quantified with ImageJ and normalized to the highest protein amount detected in each run.

Scube2 pull down. For FLAG-tagged Scube2 pull down, HEK cells were seeded into six-well plate and transfected with 1 µg Scube2 by using Polyfect (Qiagen). Cells were incubated for 2 days at 37°C with 5% CO_2. For protein pull-downs, anti-FLAG M2-agarose beads (Sigma) were used. For each pull down, 40 µL beads were added to 1 mL sample, the samples incubated over night at 4°C on a rotator and centrifuged at 8000g for 30 sec. After the supernatant was discarded, the precipitates were washed three times using 500 µL TBS. Beads were again centrifuged at 8000g for 30 sec between the washing steps and the supernatant was discarded. Proteins were then eluted from the beads using 30 µL reducing SDS buffer and were incubated for 10 min at 85°C. After centrifugation at 8000g for 30 sec, the supernatants were loaded to a 15% SDS polyacrylamide gel and proteins detected by Western blot analysis using polyclonal α-FLAG antibodies (Sigma, St. Louis, USA) and α-ApoA1 antibodies (ABIN7427912, antibodies-online.com). Note that due to the high serum conditions used in this assay, it was not possible to detect HDL-loading controls by protein precipitation and immunodetection of the sample input. Instead, we routinely confirmed identical serum concentrations in each sample by SEC of the supernatant after pulldown and spectrometric analysis, followed by immunoblotting of the eluted fractions to confirm similar levels of HDL in all samples.

Synthesis of biotinylated heparin. Biotinylated heparin was synthesized by adapting a previously reported procedure [83]. Heparin (4 mM, Sigma-Aldrich) was dissolved in 100 mM

acetate buffer (made from glacial acetic acid (Carl Roth, Karlsruhe, Germany) and sodium acetate (Sigma-Aldrich) at pH 4.5) containing aniline (100 mM, Sigma-Aldrich). Biotin-PEG_3-oxyamine (3.4 mM, Conju-Probe, San Diego, USA) was added to the heparin solution and allowed to react for 48 h at 37 °C. The final product was dialyzed against water for 48 h by using a dialysis membrane with a 3.5 kDa cutoff. The obtained biotinylated heparin was characterized by biotin-streptavidin binding assays using QCM-D. The average mass of the heparin, when anchored to the surface, was estimated at 9 kDa (~ 18 disaccharide units) by QCM-D analysis [84].

Preparation of small unilamellar vesicles (SUVs). SUVs were prepared by adapting reported procedures [85, 86]. A mixture of lipids composed of 1 mg/mL 1,2-dioleoyl-sn-glycero3-phosphocholine (DOPC, Avanti Polar Lipids) and 5 mol% of 1,2-dioleoyl-sn-glycero-3-phosphoethanolamine-N-(cap biotinyl) (DOPE-biotin, Avanti Polar Lipids) was prepared in chloroform in a glass vial. Subsequently, the solvent was evaporated with a low nitrogen stream while simultaneously turning the vial in order to obtain a homogenous lipidic film. The residual solvent was removed for 1 h under vacuum. Subsequently, the dried film was rehydrated in ultrapure water to a final concentration of 1 mg/mL and vortexed to ensure the complete solubilization of the lipids. The lipids were sonicated for about 5 min until the opaque solution turned clear. The obtained SUVs were stored in the refrigerator and used within 2 weeks.

QCM-D measurements. QCM-D measurements were performed with a QSense Analyser (Biolin Scientific, Gothenburg, Sweden) and SiO_2-coated sensors (QSX303, Biolin Scientific). The measurements were performed at 22 °C by using four parallel flow chambers and one peristaltic pump (Ismatec, Grevenbroich, Germany) with a flow rate of 75 µL per min. The normalized frequency shifts ΔF, and the dissipation shifts ΔD, were measured at six overtones (i = 3, 5, 7, 9, 11, 13). The fifth overtone (i = 5) is presented in this paper; all other overtones gave qualitatively similar results. QCM-D sensors were first cleaned by immersion in a 2 wt% sodium dodecyl sulfate solution for 30 min and subsequently rinsed with ultrapure water. The sensors were then dried under a nitrogen stream and activated by 10 min treatment with a UV/ozone cleaner (Ossila, Sheffield, UK). For the formation of supported lipid bilayers (SLBs), after obtaining a stable baseline, freshly made SUVs were diluted to a concentration of 0.1 mg/mL in buffer solution (wash buffer A, 10 mM Tris, 100 mM NaCl (Sigma Aldrich) at pH 7.4) containing 10 mM of $CaCl_2$ directly before use and flushed into the chambers. The quality of the SLBs was monitored *in situ* to ascertain high-quality SLBs were formed, corresponding to equilibrium values of $\Delta F = -24 \pm 1$ Hz and $\Delta D < 0.5 \times 10^{-6}$. Afterward, a solution of streptavidin (150 nM) was passed over the SLBs, followed by the addition of biotinylated heparin (10 µg per mL). Each sample solution was flushed over the QCM-D sensor until the signals equilibrated and subsequently rinsed with wash buffer A (see above). Before the addition of 80 µg/mL HDL and Scube2, F and D were set to 0 and the flow rate was reduced to 20 µL per min. Analysis was performed using QSoft401 version 2.7.3.883.

FACS: Bosc23 cells (a transfected HEK293 derivative) were transfected with Scube2 and a Scube2 variant lacking the major HS-binding amino acid motif, non-enzymatically removed from the culture dish by using Versene (PAA), and suspended in PBS containing 5% FCS in a

total volume of 0.5 ml. Scube2-transfected cells were incubated with heparinases I to III (AMS Biotechnology) at 37°C or with 10 µg/ml heparin (AppliChem) at 4°C for 1 h. Cells were washed and treated with α-FLAG antibody (1:500 dilution) for 1 h and fluorescein isothiocyanate-conjugated goat-α-rabbit secondary antibody (1:200 dilution, Dianova) for 30 min on ice. FACS analysis was performed on a BD Accuri C6 flow cytometer (BD Biosciences). Histograms were created by using FlowJo single cell analysis software.

Mass spectrometry. Scube2 was expressed and precipitated as before using the pull down. Samples were eluted using 0.1 M Glycine HCl pH 3.5. 100 µL 0.1 M Glycine HCl were added to each sample and incubated for 10 min at room temperature. Afterwards, samples were centrifuged at 8200g for 10 sec. Supernatants were transferred into a new tube containing 10 µL 0.5 M Tris-HCl and 1.5 M NaCl. The protein concentration was measured and the concentration was set to 50 µg per sample. DTT (Dithiothreitol) were added to the samples to a final concentration of 5 mM and incubated at 25°C for 1 h. CAA (Chloroacetamide) was added to each sample to a final concentration of 40 mM and incubated in the dark for 30 min. Last, trypsine was added to an enzyme:substrate ration of 1:75 and incubated at 25°C overnight. Samples were purified using StageTip purification. The StageTips (Thermo Fisher, 13-110-061) were equilibrated using 20 µL 100% methanol, 20 µL 0.1% fomic acid in 80% acetonitrile, and 20 µL 0.1% formic acid in water. Between each step, StageTips were centrifuged at 800g for 1 min. Afterward, the samples were centrifuged at full speed for 5 min. Next, the samples were loaded onto the StageTips. The StageTips were centrifuged at 800g for 3 min. The tips were then washed first with 30 µL 0.1% formic acid in water and centrifuged at 800g for 1 min and next twice with 30 µL 0.1 formic acid in 80% acetoniltrile. Tips were centrifuged at 800g for 1 min between washing steps. Samples were analyzed by the CECAD Proteomics Facility on an Orbitrap Exploris 480 equipped with FAIMSpro duo (granted by the German Research Foundation under INST 216/1163-1 FUGG) mass spectrometer that was coupled to an Vanquish neo in trap-and-elute setup (all Thermo Scientific). Samples were loaded onto a precolumn (Acclaim 5µm PepMap 300 µ Cartridge) with a flow of 60 µl/min before reverse-flushed onto an in-house packed analytical column (30 cm length, 75 µm inner diameter, filled with 2.7 µm Poroshell EC120 C18, Agilent). Peptides were chromatographically separated with an initial flow rate of 400 nL/min and the following gradient: initial 2% B (0.1% formic acid in 80 % acetonitrile), up to 6 % in 3 min. Then, flow was reduced to 300 nl/min and B increased to 20% B in 26 min, up to 35% B within 15 min and up to 98% solvent B within 1.0 min while again increasing the flow to 400 nl/min, followed by column wash with 95% solvent B and reequilibration to initial condition. The mass spectrometer was operated in Top24 data-dependent acquisition with MS1 scans acquired from 350 m/z to 1400 m/z at 60k resolution and an AGC target of 300%. MS2 scans were acquired at 15 k resolution with a maximum injection time of 118 ms and a normalized AGC target of 50% in a 2 Th window and a fixed first mass of 110 m/z. All MS1 scans were stored as profile, all MS2 scans as centroid. All mass spectrometric raw data were processed with Maxquant (version 2.2, [87]) using default parameters against a chimeric database consisting of the canonical Human UniProt database (UP5640, downloaded 04/01/2023) merged with 199 fetal bovine serum sequences [66]. Follow-up analysis was done in Perseus 1.6.15 [88]. Protein groups were filtered for potential contaminants and insecure identifications, and the Scube2-interacting protein candidates ranked according to the number of identified peptides.

Bioanalytical and statistical analysis. All statistical analyses were performed in GraphPad Prism. Applied statistical tests, post hoc tests, and number of independently performed experiments are stated in the figure legends. A p-value of < 0.05 was considered statistically significant. *: p<0.05, **: p<0.01, ***: p<0.001, and ****: p<0.0001 in all assays. Error bars represent the standard deviations of the means. Standard deviations as shown for Shh protein expression, and release from HEK cells on Western blots represents their variations from the average value (set to 100%) detected on the same blot.

References

1. McMahon, A.P., P.W. Ingham, and C.J. Tabin, *Developmental roles and clinical significance of hedgehog signaling.* Curr Top Dev Biol, 2003. **53**: p. 1-114.
2. Theunissen, J.W. and F.J. de Sauvage, *Paracrine Hedgehog signaling in cancer.* Cancer Res, 2009. **69**(15): p. 6007-10.
3. Yauch, R.L., et al., *A paracrine requirement for hedgehog signalling in cancer.* Nature, 2008. **455**(7211): p. 406-10.
4. Zhao, C., et al., *Hedgehog signalling is essential for maintenance of cancer stem cells in myeloid leukaemia.* Nature, 2009. **458**(7239): p. 776-9.
5. Porter, J.A., K.E. Young, and P.A. Beachy, *Cholesterol modification of hedgehog signaling proteins in animal development.* Science, 1996. **274**(5285): p. 255-9.
6. Pepinsky, R.B., et al., *Identification of a palmitic acid-modified form of human Sonic hedgehog.* J Biol Chem, 1998. **273**(22): p. 14037-45.
7. Vyas, N., et al., *Nanoscale organization of hedgehog is essential for long-range signaling.* Cell, 2008. **133**(7): p. 1214-27.
8. Bellaiche, Y., I. The, and N. Perrimon, *Tout-velu is a Drosophila homologue of the putative tumour suppressor EXT-1 and is needed for Hh diffusion.* Nature, 1998. **394**: p. 85-88.
9. Bornemann, D.J., et al., *Abrogation of heparan sulfate synthesis in Drosophila disrupts the Wingless, Hedgehog and Decapentaplegic signaling pathways.* Development, 2004. **131**(9): p. 1927-38.
10. Takei, Y., et al., *Three Drosophila EXT genes shape morphogen gradients through synthesis of heparan sulfate proteoglycans.* Development, 2004. **131**(1): p. 73-82.
11. Han, C., et al., *Drosophila glypicans control the cell-to-cell movement of Hedgehog by a dynamin-independent process.* Development, 2004. **131**(3): p. 601-11.
12. Desbordes, S.C. and B. Sanson, *The glypican Dally-like is required for Hedgehog signalling in the embryonic epidermis of Drosophila.* Development, 2003. **130**(25): p. 6245-55.
13. Ortmann, C., et al., *Sonic hedgehog processing and release are regulated by glypican heparan sulfate proteoglycans.* J Cell Sci, 2015. **128**(12): p. 2374-85.
14. Ayers, K.L., et al., *The long-range activity of Hedgehog is regulated in the apical extracellular space by the glypican Dally and the hydrolase Notum.* Dev Cell, 2010. **18**(4): p. 605-20.

15. Bilioni, A., et al., *Balancing Hedgehog, a retention and release equilibrium given by Dally, Ihog, Boi and shifted/DmWif.* Dev Biol, 2013. **376**(2): p. 198-212.
16. Jakobs, P., et al., *Bridging the gap: heparan sulfate and Scube2 assemble Sonic hedgehog release complexes at the surface of producing cells.* Sci Rep, 2016. **6**: p. 26435.
17. Hollway, G.E., et al., *Scube2 mediates Hedgehog signalling in the zebrafish embryo.* Dev Biol, 2006. **294**(1): p. 104-18.
18. Kawakami, A., et al., *The zebrafish-secreted matrix protein you/scube2 is implicated in long-range regulation of hedgehog signaling.* Curr Biol, 2005. **15**(5): p. 480-8.
19. Woods, I.G. and W.S. Talbot, *The you gene encodes an EGF-CUB protein essential for Hedgehog signaling in zebrafish.* PLoS Biol, 2005. **3**(3): p. e66.
20. Tsai, M.T., et al., *Isolation and characterization of a secreted, cell-surface glycoprotein SCUBE2 from humans.* Biochem J, 2009. **422**(1): p. 119-28.
21. Tukachinsky, H., et al., *Dispatched and scube mediate the efficient secretion of the cholesterol-modified hedgehog ligand.* Cell Rep, 2012. **2**(2): p. 308-20.
22. Creanga, A., et al., *Scube/You activity mediates release of dually lipid-modified Hedgehog signal in soluble form.* Genes Dev, 2012. **26**(12): p. 1312-25.
23. Jakobs, P., et al., *Scube2 enhances proteolytic Shh processing from the surface of Shh-producing cells.* J Cell Sci, 2014. **127**(Pt 8): p. 1726-37.
24. Lin, Y.C., et al., *The biology of SCUBE.* J Biomed Sci, 2023. **30**(1): p. 33.
25. Lee, H., et al., *BMP4 binds CUB domains of tolloids and inhibits proteinsase activity.* Genes Dev., 2009. **23**: p. 2551-62.
26. Li, L., et al., *PDGF-D prodomain differentially inhibits the biological activities of PDGF-D and PDGF-B.* J Mol Biol, 2022. **434**: p. 167709.
27. Gaboriaud, C., et al., *Assembly of C1 and the MBL- and ficolin-MASP complexes: structural insights.* Immunobiology, 2007. **212**(4-5): p. 279-88.
28. Balzar M, et al., *Epidermal growth factor-like repeats mediate lateral and reciprocal interactions of Ep-CAM molecules in homophilic adhesions.* Mol Cell Biol., 2001. **21**: p. 2570-80.
29. Ishii J, et al., *SREC-II, a new member of the scavenger receptor type F family, trans-interacts with SREC-I through its extracellular domain.* J Biol Chem, 2002. **277**: p. 39696-702.
30. Lin, Y.C., et al., *inhibition of endothelial SCUBE2 (signal peptide-CUB-EGF domain-containing protein 2), a novel VEGFR2 (vascular endothelial growth factor receptor 2) coreceptor, suppresses tumor angiogenesis.* Arterioscler Thromb Vasc Biol, 2018. **38**: p. 1202-15.
31. Lin, Y.C., et al., *Endothelial SCUBE2 interacts with VEGFR2 abd regulates VEGF-induced angiogenesis.* Arterioscler Thromb Vasc Biol, 2017. **37**: p. 144-55.
32. Liao, W.J., K.C. Tsao, and R.B. Yang, *Electrostatics and N-glycan-mediated membrane tethering of SCUBE1 is critical for promoting bone morphogenetic protein signalling.* Biochem J, 2016. **473**(5): p. 661-72.
33. Ehring, K., et al., *Conserved cholesterol-related activities of Dispatched 1 drive Sonic hedgehog shedding from the cell membrane.* J Cell Sci, 2022. **135**(5).
34. Burke, R., et al., *Dispatched, a novel sterol-sensing domain protein dedicated to the release of cholesterol-modified hedgehog from signaling cells.* Cell, 1999. **99**(7): p. 803-15.

35. Ma, Y., et al., *Hedgehog-mediated patterning of the mammalian embryo requires transporter-like function of dispatched.* Cell, 2002. **111**(1): p. 63-75.
36. Kawakami, T., et al., *Mouse dispatched mutants fail to distribute hedgehog proteins and are defective in hedgehog signaling.* Development, 2002. **129**(24): p. 5753-65.
37. Nakano, Y., et al., *Inactivation of dispatched 1 by the chameleon mutation disrupts Hedgehog signaling in the zebrafish embryo.* Dev Biol., 2004. **269**(2): p. 381-92.
38. Hall, E.T., E.R. Cleverdon, and S.K. Ogden, *Dispatching Sonic Hedgehog: Molecular Mechanisms Controlling Deployment.* Trends Cell Biol, 2019. **29**(5): p. 385-395.
39. Luo, J., H. Yang, and B.L. Song, *Mechanisms and regulation of cholesterol homeostasis.* Nat Rev Mol Cell Biol, 2020. **21**(4): p. 225-245.
40. Palm, W., et al., *Secretion and signaling activities of lipoprotein-associated hedgehog and non-sterol-modified hedgehog in flies and mammals.* PLoS Biol, 2013. **11**(3): p. e1001505.
41. Ehring, K., et al., *Two-way Dispatched function in Sonic hedgehog shedding and transfer to high-density lipoproteins.* Elife, 2024. **12**.
42. Dierker, T., et al., *Heparan sulfate-modulated, metalloprotease-mediated sonic hedgehog release from producing cells.* J Biol Chem, 2009. **284**(12): p. 8013-22.
43. Ohlig, S., et al., *Sonic hedgehog shedding results in functional activation of the solubilized protein.* Dev Cell, 2011. **20**(6): p. 764-74.
44. Damhofer, H., et al., *Blocking Hedgehog release from pancreatic cancer cells increases paracrine signaling potency.* J Cell Sci, 2015. **128**: p. 129-139.
45. Johnson, J.L., et al., *Scube activity is necessary for Hedgehog signal transduction in vivo.* Dev Biol, 2012. **368**(2): p. 193-202.
46. Panakova, D., et al., *Lipoprotein particles are required for Hedgehog and Wingless signalling.* Nature, 2005. **435**(7038): p. 58-65.
47. Gallet, A., et al., *Cholesterol modification of hedgehog is required for trafficking and movement, revealing an asymmetric cellular response to hedgehog.* Dev Cell, 2003. **4**(2): p. 191-204.
48. Gallet, A. and P.P. Therond, *Temporal modulation of the Hedgehog morphogen gradient by a patched-dependent targeting to lysosomal compartment.* Dev Biol, 2005. **277**(1): p. 51-62.
49. Gallet, A., et al., *Cholesterol modification is necessary for controlled planar long-range activity of Hedgehog in Drosophila epithelia.* Development, 2006. **133**(3): p. 407-18.
50. Chamberlain, C.E., et al., *Notochord-derived Shh concentrates in close association with the apically positioned basal body in neural target cells and forms a dynamic gradient during neural patterning.* Development, 2008. **135**(6): p. 1097-106.
51. Ma, C., et al., *The segment polarity gene hedgehog is required for progression of the morphogenetic furrow in the developing Drosophila eye.* Cell, 1993. **75**(5): p. 927-38.
52. Brand, A.H. and N. Perrimon, *Targeted gene expression as a means of altering cell fates and generating dominant phenotypes.* Development, 1993. **118**(2): p. 401-15.
53. Pan, D. and G.M. Rubin, *Kuzbanian controls proteolytic processing of Notch and mediates lateral inhibition during Drosophila and vertebrate neurogenesis.* Cell, 1997. **90**(2): p. 271-80.
54. Rogers, E.M., et al., *Pointed regulates an eye-specific transcriptional enhancer in the Drosophila hedgehog gene, which is required for the movement of the morphogenetic furrow.* Development, 2005. **132**(21): p. 4833-43.

55. Kastl, P., et al., *Disrupting Hedgehog Cardin-Weintraub sequence and positioning changes cellular differentiation and compartmentalization in vivo.* Development, 2018. **145**(18): p. dev167221.
56. Kirschke, S., et al., *The metalloprotease ADAM10 generates soluble interleukin-2 receptor alpha (sCD25) in vivo.* J Biol Chem, 2022. **298**(6): p. 101910.
57. Baran, P., et al., *Minimal interleukin 6 (IL-6) receptor stalk composition for IL-6 receptor shedding and IL-6 classic signaling.* J Biol Chem, 2013. **288**(21): p. 14756-68.
58. Riethmueller, S., et al., *Cleavage Site Localization Differentially Controls Interleukin-6 Receptor Proteolysis by ADAM10 and ADAM17.* Sci Rep, 2016. **6**: p. 25550.
59. Huovila, A.P., et al., *Shedding light on ADAM metalloproteinases.* Trends Biochem Sci, 2005. **30**(7): p. 413-22.
60. Reiss, K. and S. Bhakdi, *The plasma membrane: Penultimate regulator of ADAM sheddase function.* Biochimica Et Biophysica Acta-Molecular Cell Research, 2017. **1864**(11): p. 2082-2087.
61. Glise, B., et al., *Shifted, the Drosophila ortholog of wnt inhibitory factor-1, controls the distribution and movement of hedgehog.* Dev Cell, 2005. **8**(2): p. 255-66.
62. Gorfinkiel, N., et al., *The Drosophila ortholog of the human wnt inhibitor factor shifted controls the diffusion of lipid-modified hedgehog.* Dev Cell, 2005. **8**(2): p. 241-53.
63. Prieto JH, et al., *Dynamics of the fragment of thrombomodulin containing the fourth and fifth epidermal growth factor-like domains correlate with function.* Biochemistry, 2005. **44**: p. 1225-33.
64. Lo Surdo P, et al., *Mechanistic implications for LDL receptor degradation from the PCSK9/LDLR structure at neutral pH.* EMBO Reports, 2011. **12**: p. 1300-5.
65. Lillis, A.P., et al., *LDL receptor-related protein 1: unique tissue-specific functions revealed by selective gene knockout studies.* Physiol Rev, 2008. **88**(3): p. 887-918.
66. Shin, J., et al., *Use of composite protein database including search result sequences for mass spectrometric analysis of cell secretome.* PLoS One, 2015. **10**(3): p. e0121692.
67. Randolph, G.J. and N.E. Miller, *Lymphatic transport of high-density lipoproteins and chylomicrons.* J Clin Invest, 2014. **124**(3): p. 929-35.
68. Yamamoto, K., et al., *Novel insights into the multifaceted and tissue-specific roles of the endocytic receptor LRP1.* J Biol Chem, 2024. **300**(8): p. 107521.
69. Herz, J., et al., *Surface location and high affinity for calcium of a 500-kd liver membrane protein closely related to the LDL-receptor suggest a physiological role as lipoprotein receptor.* EMBO J, 1988. **7**(13): p. 4119-27.
70. Strickland, D.K., et al., *Sequence identity between the alpha 2-macroglobulin receptor and low density lipoprotein receptor-related protein suggests that this molecule is a multifunctional receptor.* J Biol Chem, 1990. **265**(29): p. 17401-4.
71. McCarthy, R.A., et al., *Megalin functions as an endocytic sonic hedgehog receptor.* J Biol Chem, 2002. **277**(28): p. 25660-7.
72. Lookene, A., R. Savonen, and G. Olivecrona, *Interaction of lipoproteins with heparan sulfate proteoglycans and with lipoprotein lipase. Studies by surface plasmon resonance technique.* Biochemistry, 1997. **36**: p. 5267-5275.
73. Stewart, D.P., et al., *Cleavage activates dispatched for Sonic Hedgehog ligand release.* Elife, 2018. **7**.

74. Heberlein, U., T. Wolff, and G.M. Rubin, *The TGF beta homolog dpp and the segment polarity gene hedgehog are required for propagation of a morphogenetic wave in the Drosophila retina.* Cell, 1993. **75**(5): p. 913-26.
75. Mohler, J., *Requirements for hedgehog, a segmental polarity gene, in patterning larval and adult cuticle of Drosophila.* Genetics, 1988. **120**(4): p. 1061-72.
76. Williams, K.P., et al., *Functional antagonists of sonic hedgehog reveal the importance of the N terminus for activity.* J Cell Sci, 1999. **112**: p. 4405-14.
77. Chang, S.C., et al., *Two distinct sites in sonic hedgehog combine for heparan sulfate interactions and cell signaling functions.* J Biol Chem, 2011. **286**(52): p. 44391-402.
78. Gude, F., et al., *Hedgehog is relayed through dynamic heparan sulfate interactions to shape its gradient.* Nat Commun, 2023. **14**(1): p. 758.
79. Lundberg, J., M. Rudling, and B. Angelin, *Interstitial fluid lipoproteins.* Curr Opin Lipidol, 2013. **24**(4): p. 327-31.
80. Albers, J.J., G.R. Warnick, and M.C. Chenng, *Quantitation of high density lipoproteins.* Lipids, 1978. **13**(12): p. 926-32.
81. Lin, Y.-C., et al., *Disruption of Scube2 Impairs Endochondral Bone Formation.* Journal of Bone and Mineral Research, 2015. **30**(7): p. 1255-1267.
82. Eugster, C., et al., *Lipoprotein-heparan sulfate interactions in the Hh pathway.* Dev Cell, 2007. **13**(1): p. 57-71.
83. Thakar, D., et al., *A quartz crystal microbalance method to study the terminal functionalization of glycosaminoglycans.* Chem Commun (Camb), 2014. **50**(96): p. 15148-51.
84. Srimasorn, S., et al., *A quartz crystal microbalance method to quantify the size of hyaluronan and other glycosaminoglycans on surfaces.* Sci Rep, 2022. **12**(1): p. 10980.
85. Bartelt, S.M., et al., *Dynamic blue light-switchable protein patterns on giant unilamellar vesicles.* Chem Commun (Camb), 2018. **54**(8): p. 948-951.
86. Di Iorio, D., et al., *Recruitment of receptors at supported lipid bilayers promoted by the multivalent binding of ligand-modified unilamellar vesicles.* Chem Sci, 2020. **11**(12): p. 3307-3315.
87. Tyanova, S., T. Temu, and J. Cox, *The MaxQuant computational platform for mass spectrometry-based shotgun proteomics.* Nat Protoc, 2016. **11**(12): p. 2301-2319.
88. Tyanova, S., et al., *The Perseus computational platform for comprehensive analysis of (prote)omics data.* Nat Methods, 2016. **13**(9): p. 731-40.